fuels

MDPI

Review

Evaluation of Chemical Kinetic Mechanisms for Methane Combustion: A Review from a CFD Perspective

Niklas Zettervall [1], Christer Fureby [2] and Elna J. K. Nilsson [3,*]

[1] Defense Security Systems Technology, Swedish Defense Research Agency—FOI, SE 147 25 Tumba, Sweden; niklas.zettervall@foi.se
[2] Department of Energy Sciences, Lund University, Box 118, SE 221 00 Lund, Sweden; christer.fureby@energy.lth.se
[3] Combustion Physics, Department of Physics, Lund University, Box 118, SE 221 00 Lund, Sweden
* Correspondence: elna.heimdal_nilsson@forbrf.lth.se

Abstract: Methane is an important fuel for gas turbine and gas engine combustion, and the most common fuel in fundamental combustion studies. As Computational Fluid Dynamics (CFD) modeling of combustion becomes increasingly important, so do chemical kinetic mechanisms for methane combustion. Kinetic mechanisms of different complexity exist, and the aim of this study is to review commonly used detailed, reduced, and global mechanisms of importance for CFD of methane combustion. In this review, procedures of relevance to model development are outlined. Simulations of zero and one-dimensional configurations have been performed over a wide range of conditions, including addition of H_2, CO_2 and H_2O, and the results are used in a final recommendation about the use of the different mechanisms. The aim of this review is to put focus on the importance of an informed choice of kinetic mechanism to obtain accurate results at a reasonable computational cost. It is shown that for flame simulations, a reduced mechanism with only 42 irreversible reactions gives excellent agreement with experimental data, using only 5% of the computational time as compared to the widely used GRI-Mech 3.0. The reduced mechanisms are highly suitable for flame simulations, while for ignition they tend to react too slow, giving longer than expected ignition delay time. For combustible mixtures with addition of hydrogen, carbon dioxide, or water, the detailed as well as reduced mechanisms generally show as good performance as for the corresponding simulations of pure methane/air mixtures.

Keywords: chemical kinetics; comprehensive mechanism; methane; reduced mechanism; hydrogen; detailed mechanism; CFD

Citation: Zettervall, N.; Fureby, C.; Nilsson, E.J.K. Evaluation of Chemical Kinetic Mechanisms for Methane Combustion: A Review from a CFD Perspective. *Fuels* **2021**, *2*, 210–240. https://doi.org/10.3390/fuels2020013

Academic Editor: Stephen Dooley

Received: 20 January 2021
Accepted: 18 May 2021
Published: 24 May 2021

1. Introduction

Combustion of methane, CH_4, is of significant importance in practical applications and for research purposes. Methane is a main component in biogas, as well as in fossil natural gas, and can be part of the important transition from fossil fuel to biofuel use. As the main component of natural gas methane can be considered as a relatively environmentally friendly fossil fuel, due to its advantageous combustion properties resulting in fewer harmful pollutants compared to other gaseous or liquid fossil fuels [1]. In combustion research methane is the fuel of choice in phenomenological studies due to its ease of use and wide availability. Due to its wide use and the fact that it is a relatively small fuel molecule the chemical kinetics of methane combustion is fairly well understood [2], at least compared to the significantly larger and more complex fuel molecules that are components of diesel or gasoline. Detailed chemical kinetics mechanisms for methane/air combustion are capable of predicting combustion characteristics over a wide range of conditions with respect to temperature, pressure and equivalence ratio, even though there still are quite large uncertainties at extreme conditions of low temperature and/or high pressure of many real combustion applications. Methane is also the fuel for which the largest number of

simplified kinetic mechanisms, for use in Computational Fluid Dynamic (CFD) simulations, have been developed.

To further improve the understanding of methane combustion and to develop the industrial combustion systems, CFD simulations with explicit chemistry are needed [3]. Due to limitations in computational capacity, modeling has mainly been performed with highly simplified chemical descriptions, so-called global chemistry, or the flamelet approach [4]. These methods do not, however, resolve the interactions between chemistry and turbulence on the smallest scales [5]. They are also not useful for characterization of pollutant formation, an aspect that becomes increasingly important as a result of environmental concerns [6]. Large Eddy Simulations (LES) are suitable for the modeling of turbulent combustion coupled with chemical kinetics, but due to the computational cost implementation of highly detailed kinetic schemes is not feasible. With the current computational capacity and LES modeling approaches, kinetic mechanisms of about 20–30 species and 80–100 reactions represent an upper limit in terms of mechanism size. It has been shown that this number of species is adequate to model important combustion characteristics of common hydrocarbon fuels [5].

The choice of mechanism for a CFD simulation is limited by the need for short computational time and varying demands with respect to output parameters, depending on the task at hand. The community of researchers with expertise in CFD simulations are, commonly, not experts in chemical kinetics modeling. Unfortunately, lack of knowledge among CFD experts or lack of communication between kineticists and CFD scientists, sometimes results in poor choice of mechanism for CFD simulations. Expert assessment of kinetic mechanisms needs to be made available for CFD scientists, to ensure that the most suitable mechanisms are incorporated in CFD simulations.

As CFD simulations are becoming increasingly important in the development of industrial burners and engines the requirements on the models may change compared to pure research cases. An example of this is that in idealized laboratory research systems or simulations the combustible mixture commonly consists of only one fuel component and the oxidizer. Most kinetic mechanisms are developed for pure fuels burning in dry air. However, in a real system there might be elevated levels of water vapor and exhaust gas recirculation increasing the levels of CO_2 [7]. Methane is the dominating component of natural gas, biogas, and bio-syngas [7–10], fuels that also contain one or several of CO_2, CO, H_2, higher hydrocarbons and possibly also the inert N_2. In addition, a real system is never completely dry, but H_2O will be present to different extent depending on temperature and other conditions. In Table 1, common compositions that can be encountered in a real system are listed [7–10]. Natural gas is exemplified by two quite extreme cases considering methane content [10], but also a typical range of compositions as specified by Uniongas.

Table 1. Composition of relevant fuel mixtures incorporating methane, in volume-%. "High HC" stands for Higher Hydrocarbons, i.e., with two carbon atoms or more.

	Natural Gas			Biogas [7,8]	Bio-Syngas [7,9]
Fuel Components	**Typical Range** [a]	**Frigg (North Sea) [10]**	**Lacq (France) [10]**		
CH_4	87–97	95.7	69.2	50–75	8–11
H_2	Trace	-	-	0–1	22–32
CO_2	0.05–1	0.3	9.3	25–50	21–30
CO	-	-	-	-	28–36
High HC	1.5–10	3.6	5.2	-	-

[a] https://www.uniongas.com/about-us/about-natural-gas/chemical-composition-of-natural-gas (accessed on 1 August 2018).

Natural gas, and therefore methane, is the dominating fuel in gas turbines [11]. In recent years there has been an increasing interest in co-firing natural gas with hydrogen, H_2, in gas turbines. This is motivated by the fact that hydrogen is a carbon-free energy carrier but also because it affects the flame properties and allow combustion at leaner conditions [12]. Extensive research on combustion of methane/hydrogen blends has

been performed on all scales, from idealized laboratory flames [12] to real gas turbine burners [13–15]. As reviewed by Tang et al. [16], hydrogen addition to a hydrocarbon fuel result in increased chemical reactivity giving a shortened ignition delay time and an increased flammability range. The same group published an analysis of the effects of hydrogen addition on the laminar flame speed of a hydrocarbon [16] investigating the kinetic, thermal, and diffusion effects, concluding that the kinetic effects dominated. There is also an increasing interest to use natural gas in Compression Ignition (CI) engines, commonly in a dual fuel system together with Diesel. Recently there have been significant improvement in predictive capability in modeling of dual fuel engines with natural gas (methane as main component), and in this context we like to highlight the works of research groups at Graz University [17] and Istituto Motori [18,19] who validated modeling approaches that advance the development of these engines.

Experimental studies on laminar burning velocities of hydrocarbons have been reviewed by, among others, Konnov et al. [20] and Ranzi et al. [21], while mixtures of hydrocarbons with hydrogen were considered in the review by Tang et al. [12]. These publications include detailed discussions on flame chemistry, of relevance to development and performance of comprehensive kinetic mechanisms. The curious reader who wants a more thorough understanding of flame chemistry and laminar flame speed is encouraged to read these works.

As already mentioned, chemical kinetic mechanisms are most often aimed at modeling of pure fuel/oxidizer mixtures in ideal laboratory systems. However, mechanisms that are validated also for mixtures of fuel with water or carbon dioxide are few. While in the ideal case the pure systems should be understood in large detail before more complicated gas mixtures are addressed, this is not a realistic approach, considering the need for simulation of complex systems. Fisher and Jiang [7] conclude in their analysis of ignition delay simulation results that the chemical kinetics of methane combustion combined with H_2, CO, or CO_2 is not yet fully understood, and that also highly detailed mechanisms are unable to accurately represent the chemistry. However, despite the fact that the understanding of combustion chemistry is far from complete there is a need for simplified kinetic schemes for implementation in CFD simulations.

The aim of the present study is to give an overview of common mechanisms for methane combustion, evaluate their performance, and discuss their potential use in CFD modeling. As part of the evaluation of the mechanisms, CPU time for 1D flame simulations is used as a metric for the computational cost. Mechanisms on all levels of complexity, from highly detailed to global, are compared with respect to performance for prediction of combustion properties related to ignition, propagation, and extinction phenomena. It is not an exhaustive review, but the aim is to include mechanisms that have been extensively referenced in the CFD literature, and the evaluation of these acts as a foundation for a general discussion. Particular focus is on reduced mechanisms that are small enough to be used in finite rate combustion LES, but with high enough detail in the chemistry to predict combustion characteristics sensitive to chemistry. This includes an ability to predict formation of major products (CO, CO_2, H_2, H_2O) and a range of intermediate species (for example CH_2O, CH, OH). To investigate the comprehensiveness of the mechanisms they are not only investigated for their performance in CH_4/air combustion but also for the fuels mixtures containing the smaller fuels CO and H_2 that are inevitably part of any hydrocarbon mechanism. The applicability of the mechanisms is further tested for relevant real-world conditions by simulating flames with elevated levels of CO_2 and H_2O.

The outline of this paper is as follows: first an overview of important concepts and development of kinetic mechanism is given, including relevant aspects of experimental data used for model development. Then, existing kinetic mechanisms of different levels of complexity are presented. The main part of the paper is the extensive validation and evaluation of the kinetic mechanisms, where methane/air combustion over an extensive range of conditions is first presented, followed by results for addition of H_2, CO_2 and

H_2O, and even syngas combustion. Finally, an overview of mechanism performance and recommendations for use of the mechanisms are presented.

With the present work we provide the modeling community with a roadmap in the selection of existing mechanisms, by pointing out strengths and weaknesses of the common mechanisms in the literature. We also highlight the important aspects to consider in further development and use of simplified chemical kinetics schemes, based on the understanding gained from existing mechanisms.

2. An Overview of Kinetic Mechanism Development

In this section the framework for mechanism development is explained, starting with definitions of common concepts. Experimental methods and the resulting data used for mechanism development are then outlined, to give the reader a basic understanding of chemical kinetics research. The explanations of the combustion characteristics and experimental methods are not exhaustive, but references are given to guide the reader to more detailed treatments of the topics.

2.1. Concepts and Definitions

Chemical kinetics mechanisms and their use in simulations are important tools in development of a fundamental understanding of combustion. Mechanisms of different complexity, including from a single reaction to tens of thousands of chemical reactions, are used depending on the need and the available computational resources. In the literature terms like "detailed", "skeletal", and "reduced" are used to indicate the level of complexity of a mechanism. Some of these terms are used ambiguously and to avoid misinterpretations the present section begins with definitions, used throughout this work. The definitions are largely adopted from Hilbert et al. [6] and Fiorina et al. [4].

In complete chemical kinetic schemes, all possible reactions of the fuel and all intermediates are included, represented by accurate reaction rate constants describing the temperature and pressure dependence. However, since knowledge about every single reaction is not available, and all known reaction rate parameters have some uncertainty, a truly complete mechanism does not exist. A complete mechanism is, in theory, expected to be comprehensive, i.e., to accurately reproduce all possible combustion cases at all relevant conditions. The broader term detailed mechanism is more commonly used, including schemes that aim at being complete but also those where some simplifications have been made on purpose and that are not expected to be fully comprehensive. An aspect of true comprehensiveness is that a mechanism should be accurate for the full fuel hierarchy, which mean that a mechanism for methane combustion should also accurately predict combustion of the smaller fuels, CO and H_2. An example of a comprehensive mechanism is AramcoMech from NUI Galway, which has been published in three versions since 2013 [22–24]. Another comprehensive detailed mechanism is that of the group at Politecnico de Milano [25], who also publish lumped versions of several mechanisms for large fuels. More detail on the structure and applicability of these detailed mechanisms are given in Section 3.2. For further insight into construction of detailed mechanisms we refer to the insightful description by H. Curran [26].

Skeletal mechanism is a kinetics scheme that consists of an intact sequence of elementary reactions from fuel to final products. The comprehensiveness of skeletal mechanisms is restricted, to various extent. Automated reduction procedures based on, for example, sensitivity analysis, are used to produce skeletal mechanisms based on extensive detailed mechanisms. Skeletal mechanism includes quite large mechanisms with thousands of reactions, but also some small schemes of hundreds of reactions or less. An example of an extensive mechanism that is denoted skeletal is the mechanism named POLIMI, by Ranzi et al. [21].

Further simplification of a mechanism gives the reduced schemes that include simplifications in the reaction path, by for example lumping of several elementary reactions. A range of automatic reduction strategies exist, commonly including steps of first mak-

ing a skeletal mechanism and then further reduce it by lumping or other procedures, as explained by Turanyi and Tomlin [27].

Global kinetic schemes use a few reactions to transform the fuel into final products, often via CO but with no further chemical details. Number of reactions are most commonly in the range 1–4, and up to ten for large fuels. Semi-global approaches are of importance for reduced mechanisms of large fuel components, in these the fuel breakdown is treated with a few global steps, while the chemistry of small species is more detailed, as exemplified by recently developed reduced mechanisms for kerosene combustion [28,29].

2.2. Target Combustion Characteristics for Mechanism Development

The first step of mechanism development, at least for the detailed schemes, is compilation of chemical reactions and their reaction rate coefficients. Kinetic data is available from dedicated experimental and computational studies that provide reaction rate coefficients, their temperature and pressure dependence, and possibly information on branching to different products. The kinetic mechanism is then executed and validated against laboratory data for macroscopic properties, where the most important are ignition delay time, flame propagation (laminar burning velocity) and extinction strain rate. In the following subsections combustion characteristics of wide use in mechanism development are outlined, including discussions on experimental uncertainties, since these are important in the comparison between experiments and modelling. The chemistry governing the combustion characteristics are also introduced, to act as a common starting point for the discussion of the different mechanisms in the validation section.

2.2.1. Premixed Auto-Ignition

Shock tube ignition experiments of premixed gases are in theory homogeneous and zero-dimensional, and solely determined by chemical kinetics. This is a good approximation at high temperature conditions, while at lower temperatures the assumption of homogeneity is not valid [7]. However, despite the uncertainties at lower temperatures, shock tube experiments, including both ignition delay time determination and species composition, are highly suitable for mechanism development. However, it is important for the mechanism development scientist to be aware that at the lower reactivity (low temperature range) conditions, where inhomogeneity and boundary layer effects may occur in the experimental system, modeling is less straightforward and the common assumptions in ignition delay modeling can give erroneous results. Analysis by Davidson and Hanson [30] show that ignition delay times from shock tubes are less reliable if they are shorter than about 50 ϕs or longer than several milliseconds, and the user of shock tube data should have this in mind when comparing modelling and experiments. The ignition can be measured using different characteristics, a common one being the rapid rise in OH concentration, or luminosity measurements from other species like CH. Different definitions of ignition delay time may give slightly different results, but as investigated by Davidson and Hanson the results based on different definitions are commonly still smaller than other experimental uncertainties. For model development it is most advisable to use the same definition of ignition delay time as in the experiments used for validation.

Other experimental setups for investigations of ignition events are Rapid Compression Machines (RCM) and counter flow flame configurations, both are important for achieving a broad range of data. RCMs are suitable for determination of low temperature ignition, which technically involves device simulating a single compression stroke of an internal combustion engine [31,32]. Counter flow flames are setups where non-premixed ignition of the fuel counter-flowing with a heated oxidizer jet is measured [33].

The chemistry of ignition is to a large extent dependent on the availability of H atoms, and the main chain branching reaction governing the reactivity of the system is $H + O_2 = O + OH$.

The competing reactions decreasing the reactivity is to a large extent chain terminating reactions removing H and thus both directly and indirectly decreasing the radical pool.

Particularly important reactions are those of H with CH_3, O_2, and OH, third body reactions that will decrease the overall reactivity of the system at elevated pressures. The pressure dependence of ignition events is, however, highly non-linear and at pressures beyond about 20 atm reactions involving HO_2/H_2O_2 system and recombination reactions of CH_3 become increasingly important. HCO radicals are among the important reactions at lower (<10 atm) pressures but has no significance at higher pressures.

The importance of both accurate pressure dependences in the chemical reactions and description of transport phenomena is apparent when considering an example of hydrogen ignition given by Law [34]. Hydrogen gas counter-flowing with heated air at 1 atm and 10 atm are shown to occur by very different mechanisms; at the low pressure radical runaway is the key process while at the higher pressure thermal runaway in the presence of diffusive transport.

Detailed chemical kinetic mechanisms commonly include the extensive chemistry required to accurately predict ignition events over a wide range of temperatures and pressure. For smaller fuel molecules such as methane the understanding of the chemical reactions is good, and the mechanisms reproduce the experimental results. Reduced chemical mechanisms with less than 50 reactions for methane can hardly include all the relevant chemistry over a wide range of conditions, they can however be tailored to give excellent results over a limited range of conditions. The global mechanisms are made for flame propagation and do not include sufficient chemistry for simulation of ignition events.

2.2.2. Flame Propagation

Laminar flames serve as the basis for fundamental principles of flame theory and is a key to understanding of complex combustion phenomena such as flame front instabilities, extinction, and turbulence, as explained by Law [34]. The fundamental parameter describing flame propagation is the laminar burning velocity, a macroscopic property of a propagating flame, governing information on high temperature chemistry.

Flame chemistry is quite similar for all hydrocarbon fuels, dominated by reactions of small molecules and radicals involving O, H, and only one C. Flame propagation is to a large extent a competition between production and destruction of reactive radicals, where a large radical pool increases the reactivity and therefore also the laminar burning velocity. Due to the relative simplicity of the governing chemistry, chemical kinetics mechanisms of all sizes can accurately reproduce laminar burning velocity, even though the applicable range of conditions decrease as mechanism size decreases.

Laminar burning velocity can be determined using several methods, suitable at different conditions. The most common methods are burner stabilized flames, spherical flames, and counter flow flames, and for an overview of these methods and information on less common methods we refer to Egolfopoulos et al. [35]. Burner stabilized flames using the heat flux method at pressures 1–5 bar [36] have the advantage that laminar burning velocity is determined on an un-stretched flame and therefore no stretch corrections need to be applied, as evaluated by Alekseev et al. [37]. A wider range of pressures is reached using outwardly propagating flame methods, but for these it is important to consider correct treatment of stretch effects and other sources of uncertainties, as discussed by Chen [38].

Experimentally determined laminar burning velocities have been reported and reviewed in several comprehensive works in recent years, for example the combined experimental review and modelling update by Ranzi et al. [39] for hydrocarbon and oxygenated fuels, and the extensive review of hydrogen, alkanes, and alcohols by Konnov et al. [20].

2.2.3. Flame Extinction

Flame extinction is a high temperature phenomenon, just like flame propagation, but the chemical kinetics governing extinction is not necessarily the same [40,41]. As demonstrated by Franzelli et al. [42] a kinetic scheme needs to accurately predict both laminar flame propagation and extinction strain rate to be of use in turbulent combustion simulations (LES).

It has been shown that a kinetic mechanism that gives accurate laminar burning velocity may not be able to reproduce experimental data for extinction strain rate. However, small fuels like methane extinction are mainly sensitive to the same reactions as the laminar burning velocity. Since extinction of non-premixed flames in a counter flow burner are sensitive to both chemical kinetics and transport, these flames are valuable for investigation of the coupling of the properties.

3. Selected Kinetic Mechanisms

In this section, commonly used mechanisms of different level of complexity are presented and separated into sections about detailed, global, and reduced mechanisms. Figures 1 and 2 present simulation data for laminar flames at standard conditions (1 atm, 300 K) and ignition delay time at atmospheric pressure, from the mechanisms that will be evaluated further in the later part of this paper. These initial figures allow brief discussions on general trends in capability of the mechanisms of different complexity.

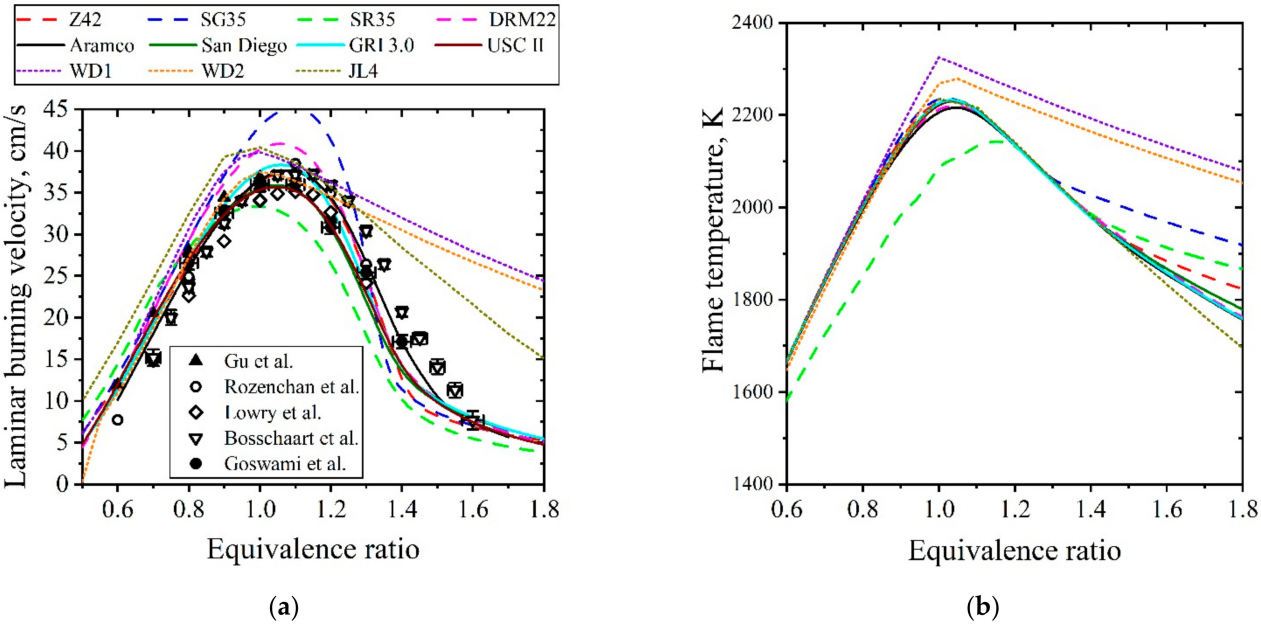

Figure 1. Simulation results for laminar burning velocities (**a**) and flame temperature (**b**) for methane/air flames at 298 K and 1 atm. Experiments are represented by symbols [36,43–46]. References to mechanisms are given in Tables 2–4.

First, however, a note about these "standard conditions" at which the bulk of the experimental data is obtained. For obvious reasons atmospheric pressure and room temperature are often the easiest conditions to study experimentally in the lab, since it involves no complications related to heating or pressure control. Therefore, the standard conditions are of significant importance for fundamental studies of combustion characteristics. Real world combustion devices like engines and furnaces do mostly operate at elevated pressures and with pre-heating of fuel and oxidizer, which mean that chemical kinetic mechanisms implemented in simulations of these applications must be able to accurately represent the relevant temperature and pressure. Chemical kinetics is strongly dependent on both temperature and pressure and this gap between what is mainly studied in the lab and the need related to "real world" applications is one of the significant challenges for the chemical kinetics and CFD communities. In this work we will address this issue in the final discussions section, but already here we want to point at the important fact: A simple kinetic mechanism that performs well under the standard conditions presented in Figures 1 and 2 may not be suitable for use in your CFD simulation of a combustion device.

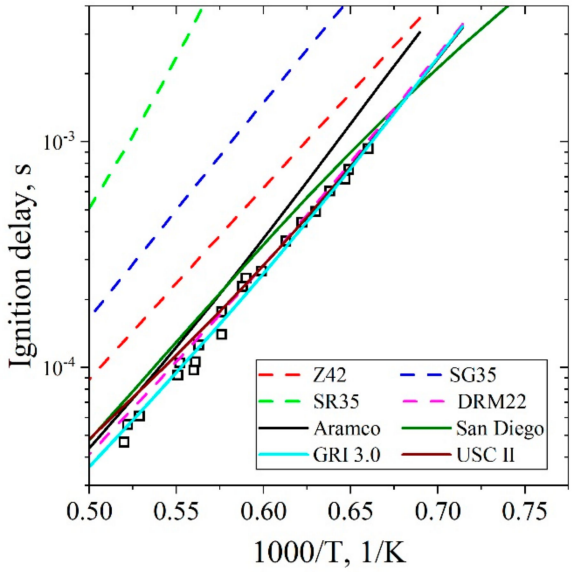

Figure 2. Shock tube ignition delay times over the temperature range 1300–2000 K at pressures of 1 atm, for stoichiometric conditions. Symbols are experiments from Hu et al. [47].

3.1. Detailed Mechanisms

Detailed kinetic mechanisms evaluated here are listed in Table 2, all these mechanisms are validated to a wide range of experimental data including velocity and composition of laminar flames, ignition delay time measurements, and oxidation in various types of reactors. As the benchmark there is the state-of-the-art detailed mechanism Aramco Mech, likely the most comprehensive mechanism for C_0-C_4 species currently available [22–24]. This mechanism is developed for a wide range of fuels and is validated to essentially all conditions for which experimental data exist, with particular focus on ignition delay. In the present work the version Aramco 2.0 is considered a benchmark for the combustion characteristics evaluated here. Other well-known mechanisms of high level of detail include GRI-Mech 3.0 (GRI 3.0) [48], USC Mech version II (USCII) [49], and the so-called San Diego mechanism (SD) [50]. These detailed mechanisms are all developed for natural gas combustion, meaning that they include methane, ethane, and propane. Many smaller mechanisms are reduced versions of the mentioned detailed mechanisms.

Figure 1 shows modelled laminar burning velocities at standard conditions, together with selected experimental data, where the full drawn lines represent the detailed mechanisms. The four detailed mechanisms are in very good agreement for both laminar burning velocity (Figure 1a) and flame temperature (Figure 1b). The differences in laminar burning velocity are for stoichiometric and moderately rich conditions up to 3 cm/s, but considering the scatter in experimental data at these conditions no significance can be given to the difference between the mechanisms. Figure 2 also reveals agreement for ignition delay time, in particular at the higher temperatures.

The detailed mechanisms have been compared and evaluated in several published works [7,47]. Hu et al. [47] conducted laminar burning velocity and ignition delay time determinations at elevated temperatures and pressure, and used the data to evaluate the mechanisms USCII, SD, and GRI 3.0 also included in the present work, and an earlier version of the Aramco mechanism. Regarding ignition delay times, Hu et al. conclude that the four mechanisms are in agreement with experiments at lower pressures and in particular for lean and stoichiometric conditions, but less so at rich conditions and high pressures. Fischer and Jiang [7] performed a comparative modeling study of ignition delay times of fuel mixtures containing CH_4, CO, H_2, and CO_2, in an effort to evaluate the performance of several kinetic schemes, including GRI 3.0, DRM22 [51], and an earlier version of the Aramco mechanism. They also show that poor modeling results are often related to reactions in the HO_2-H_2O_2 subset and point at the experimental uncertainties

for low temperature experiments. The Aramco mechanism and earlier versions from the University of Galway have been shown to be superior to GRI 3.0 and other mechanisms for prediction of ignition delay at high pressure [7], which is likely a result of recent data for chemical reactions having been used, and that a large dataset of high-pressure ignition delay times was used during mechanism development and validation.

Table 2. Detailed mechanisms for methane combustion included in the current evaluation.

Name	Ref	Fuel	No. of Species	No. of Reactions
Aramco	[22–24]	C_0-C_4, including oxygenates (2.0)	493	5131
GRI 3.0	[52]	CH_4, Natural gas	53	325
San Diego	[50]	CH_4, Natural gas	56	235
USCII	[49]	H_2/CO/C_1-C_4	111	784

As described above, the mechanisms have mainly been analyzed and compared for combustion cases with pure methane as the fuel, but there is no extensive comparison of their performance for methane with addition of the other constituents that are the target of the present work. In the mechanism evaluation part of this paper, this will therefore be discussed in some more detail.

3.2. Global Mechanisms

Global mechanisms are crude simplifications tuned to give accurate estimations of heat release, laminar flame propagation, fuel breakdown, and production of major species, within a limited range of conditions. These simplified mechanisms do, unfortunately, not capture the chemical kinetic effects governing re-ignition and extinction processes. Therefore, the global mechanisms have limited capability in simulations of, for example, lean premixed gas turbine combustion operated at high turbulence and near the lean flammability limit. However, for complex and computationally demanding systems, in particular for DNS, the global mechanisms are still the only affordable possibility and there is a continuous development of improved global schemes for various applications. Compared to tabulation methods the global mechanisms can be advantageous, since they are computationally cheaper and give accurate combustor exit temperatures and formation of a few main pollutants.

A selection of global kinetic schemes is given in Table 3, including mainly mechanisms that have been extensively used in CFD simulations during several decades, but also a few examples of recent improved mechanisms.

Table 3. Global mechanisms for CH_4/air combustion. Irrev and rev means irreversible and reversible reactions, respectively.

Name	Ref	No. of Species	No. of Reactions	Development Conditions	Validation Targets
WD1	[53,54]	4	1 irrev	1 bar, 300 K, ϕ = 0.5–1.5	T_{ad}, S_L
WD2	[53,54]	5	3 irrev	1 bar, 300 K, ϕ = 0.5–1.5	T_{ad}, S_L
JL4	[55]	6	2 irrev + 2 rev		Species profiles, premixed and diffusion flames
Seshadri	[56]	7	4 rev	1 bar, 300 K, ϕ = 1–1.4	Flame structure
Williams	[57]	4	1 irrev	1 bar, 300 K, ϕ = 0.5–1.5	T_{ad}, S_L, σ_{ext} (ϕ < 1)
Nikolaou	[58,59]	9	5 irrev		S_L, τ_{ig}, flame structure

The most used global mechanisms are likely the 1- and 2-step mechanisms developed in the early 1980s by Westbrook and Dryer (WD1 and WD2) [53,54], and the 4-step mechanisms by Jones and Lindstedt (JL4) [55] and the group of Peters [56]. A one step mechanism consists of the global combustion reaction transforming fuel to carbon dioxide and water, in a reaction with molecular oxygen. Two step mechanisms include carbon monoxide as a product from fuel oxidation and can therefore be parameterized to predict this important pollutant. These extremely simplified descriptions can with accurate tuning

predict laminar burning velocities at lean conditions, but to reach the same goal at rich conditions further complexity need to be added. The 4-step schemes include in the range five to nine species also, one of them being molecular hydrogen, which Seshadri et al. [56] showed to significantly improve the global schemes at moderately rich conditions.

Figure 1 include laminar burning velocity and flame temperature for the three highly cited mechanisms WD1, WD2, and JL4. It is clearly seen that the mechanisms fail to reproduce laminar burning velocities at rich conditions, and for WD1 and WD2 the flame temperatures are also unreasonable, while JL4 obviously gives a better representation of the heat release. None of these global mechanisms can be used to model ignition delay time.

Global mechanisms have the drawback of being limited to a narrow set of the conditions with respect to pressure, inlet temperature, and gas mixture composition. Extension to a wide range of conditions requires advanced parameterization of the reaction rate expressions. Abou-Taouk et al. [60] present a 4-step scheme (M4) optimized towards the detailed GRI 3.0 over a range of conditions. The mechanisms consist of an irreversible fuel breakdown step and three reversible reactions, which makes it effectively larger than for example the JL4 that has two irreversible fuel breakdown steps and two equilibrium reactions. In a comparative study with both laminar flame calculations and CFD of a gas turbine configuration, the M4 scheme is shown to give superior performance compared to the simpler WD2 mechanism. Recently published global schemes are based on the same chemical considerations as the early versions (f ex WD1 and WD2), but the main improvement is in the more advanced optimization of reaction rate parameters. This is exemplified by the schemes of Peters and Seshadri that include the same species and reactions, but where the latter perform significantly better at rich conditions due to a better parameterization, as investigated by Franzelli et al. [42].

The group of Williams [57] attempt to advance the 1-step global mechanisms methodology by an improved parameterization taking the heat of reaction, activation temperature and pre-exponential factors into account. Compared to earlier 1-step mechanisms, this approach also shows improved predictions of flame propagation and extinction at rich conditions. It is, however, important to note that the mechanism is developed for atmospheric pressure only.

Global schemes have mainly been constructed for methane–air combustion, but in recent years the methodology has been extended to more complex fuel mixtures, like the 5-step wet methane-syngas mixture presented by Nikolaou et al., tested towards laboratory flame and ignition targets [58], as well as evaluated in DNS [59]. The results are reported to be in reasonable agreement with more extensive mechanisms and experiments, but the mechanism has not yet been widely used.

In all use of global mechanisms, it cannot be stressed enough that the user has to be aware of the conditions that the scheme is constructed for. A global mechanism can make accurate predictions of a limited set of combustion characteristics, but only within the range of pressures, temperatures, compositions, and equivalence ratios used in the tuning of the reaction rate constants. Another important aspect investigated in recent years is that accurate predictions of laminar burning velocity is not sufficient for a mechanism that is to be used in turbulent combustion simulations, but also strain rates need to be considered in mechanism development.

3.3. Reduced Mechanisms

As is apparent from previous sections, the global mechanisms have a very limited use since they are not able to capture a range of conditions with respect to, for example, pressure. For CFD simulations of real combustion systems, there is a need for small but versatile mechanisms that can accurately model over a range of conditions that can occur during a single combustion event. Figure 3 presents an example of the important carbon containing components and the reaction paths connecting them, in a reduced (Z42) and detailed (San Diego) mechanism. For Z42 all C-species in the mechanism are included in the figure, while for San Diego only the 12 most important C-species are included.

Both these mechanisms accurately reproduce laminar burning velocities for methane/air combustion at the investigated conditions.

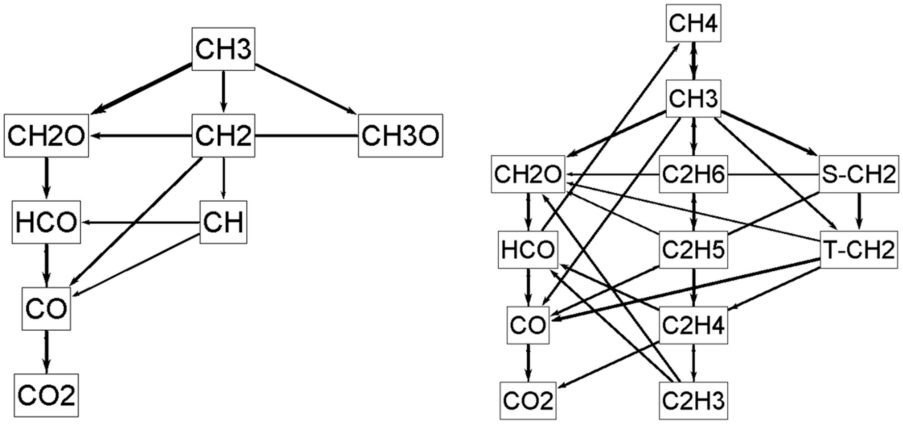

(**a**) (**b**)

Figure 3. Reaction path diagrams for the most important C-species in (**a**) Z42 and (**b**) San Diego, for laminar flames at ϕ = 1.1, 1 atm and 300 K. Diagrams are representing an unburnt fuel fraction of 0.25.

For large fuel molecules the extensive mechanisms used for 0D and 1D simulations are often of a skeletal type, since the detailed mechanisms are too large to be useful even for premixed laminar flame simulations. An example of this is the mechanism of Ranzi et al. [21], covering a range of fuels of different sizes. For a small fuel like methane the distinction between a skeletal and a reduced mechanism is less important, since a skeletal mechanism can be sufficiently small for implementation in LES.

The combustion of methane can be modelled in detail with mechanisms of the size of several hundred reactions, as evident from Table 2. To reduce the size to about a tenth of that size, to achieve the reduced mechanisms in Table 4 is an exercise that does not require advanced reduction techniques. Instead, several important reduced methane mechanisms are constructed from careful selection of most important reactions from more extensive mechanisms. The mechanisms evaluated here have been developed for particular ranges of conditions, and ideally should not be used outside those ranges. However, it is common in CFD simulations that conditions are highly varying, with the same simulated system including zones of both lean and rich combustion, and variations in temperature and pressure. Therefore, we find it important to evaluate the mechanisms over the full range of conditions that the CFD modeler may need to use a mechanism for. An extensively used reduced mechanism for methane/air combustion is the 16 species and 35 irreversible reactions mechanism by Smooke and Giovangigli (SG35), published in 1991 [61] and constructed from a selection of reactions from detailed reaction mechanisms available at the time. The mechanism was developed to model laminar flames and has been used in numerous published CFD modeling studies, for example by Bulat et al. [62]. The more recent reduced methane/air mechanism presented by Larsson et al. [63,64], called Z42, is an extension and improvement of SG35. The SG35 mechanism is known to have limited capacity at fuel rich conditions and to mitigate this a subset consisting of seven irreversible CH/CH_2 reactions from Glassman and Yetter [1] were included together with rate adjustments for the reaction paths forming CO_2 from CO. Reaction rate optimization was performed targeting global properties laminar burning velocity (S_L), flame temperature (T_{flame}), ignition delay time (τ_{ign}), and major species concentrations (CO, CO_2, H_2, H_2O) for the laminar flames. To extend the applicability of the Z42 mechanism to hydrogen combustion three reactions can be added, taken from the hydrogen mechanism by Zettervall et al. [65], resulting in a mechanism that in the present work is called Z45. The

Z42 base mechanism act as the C1-base for several reduced mechanisms for combustion of larger fuels; propane [66], kerosene [28,67], and ethylene [68], but with additional tuning of some reaction rate constants.

The mechanism for methane/hydrogen/air combustion published by Sher and Refael [69,70] consists of selected reactions from the mechanism of Pitz and Westbrook [71]. The reduced mechanism uses 34 irreversible reactions to model the direct decomposition and oxidation of fuel and one additional reaction for C_2H_6 decomposition. It is a reaction of two methyl radicals that lead to production of C_2H_6, which is treated with one global reaction to produce CH_2 and CO. This could possibly be interesting in cases when soot formation needs to be estimated, since it occurs via initial recombination of methyl radicals. In addition to these 35 reactions four more reactions are presented, these include HO_2/H_2O_2 and the authors mention they might be needed to model auto-ignition. In the following the mechanism of Sher and Refael is called SR35 or SR39, depending on the version used.

Two skeletal mechanism constructed from GRI Mech 1.2 [72,73], using a reduction method described by Wang and Frenklach [74], are DRM22 [51] that consist of 22 species and 104 reversible reactions and the slightly smaller DRM19 [75] of 19 species and 84 reversible reactions. Please note that the number of species for DRM mechanisms refer to chemically active species, in both mechanisms the inert species N_2 and Ar are also included, giving total number of species in DRM19 and DRM2 to be 21 and 24 species, respectively. DRM22 predict high-temperature ignition delay times up to 10 atm and laminar flame properties up to 20 atm. Deviations from the original mechanism GRI Mech 1.2 are in the range 1–10%, with the largest deviations at high pressures. DRM19 has larger deviation from the reference mechanism, in particular at rich conditions, and we chose to look closer at DRM22 in the present evaluation.

Table 4. Reduced and small skeletal mechanisms for CH_4/H_2/air combustion.

Name	Ref	Fuel	No. of Species	No. of Reactions	Development Conditions	Validation Targets
SG35	[61]	CH_4	16	35 irrev		S_L,
Z42/45	[63,64]	CH_4, $CH_4 + H_2$	18	42 + 3 irrev	S_L: 0.5–40 atm; 300–750 K; ϕ = 0.5–1.8 τ_{ig}: 1 atm; 300 K; ϕ = 1.0	S_L, Flame structure, τ_{ig}, σ_{ext}
SR35/39	[69,70]	CH_4, $CH_4 + H_2$	17	35 + 4 irrev	S_L: 0.8–20 atm; 280–650 K; ϕ = 0.4–1.5; 0–25 mass% H_2	S_L, Flame structure
DRM19	[75]	CH_4	19	84	S_L: 1, 20 atm; 300, 400 K; ϕ = 0.6–1.5 τ_{ig}: 0.1–50 atm; 1300–2500 K; ϕ = 0.2–2.0	S_L, τ_{ig},
DRM22	[51]	CH_4	22	104	S_L: 1, 20 atm; 300, 400 K; ϕ = 0.6–1.5 τ_{ig}: 0.1–50 atm; 1300–2500 K; ϕ = 0.2–2.0	S_L, τ_{ig},

In Figure 1a we can see that the laminar burning velocities at standard conditions are in agreement with detailed mechanisms for Z42 and DRM22, while SG35 and SR35 diverge around stoichiometry. Flame temperatures in Figure 1b are well represented up to moderately rich conditions for all mechanisms except SR35, with the largest reduced mechanism, DRM22, in close agreement with detailed mechanisms. Figure 2 shows that the three small reduced mechanisms are not reactive enough when it comes to ignition, giving ignition delay times that are too long.

In recent years a large number of reduced methane combustion mechanisms (for example see references [76,77]) have been constructed, including mechanisms tailored to treat CO_2-enriched flames, flames with significant H_2O content and mixtures with syngas (CO and H_2). Among the reduced mechanisms suitable for finite rate combustion LES, the chemical reactions are to a large extent the same, but with some important differences that may affect the choice of mechanism for different applications.

4. Modeling Details

For the detailed mechanisms and DRM22 transport and thermochemistry data were provided with the mechanism's files. For Z42, SG35, and SR35/39, mechanisms thermochemistry data from the most recent database of Goos et al. [78] was used, and transport data from the GRI 3.0 mechanism [48].

CHEMKIN PRO [79] was used to simulate laminar premixed flames, counter flow flame extinction, and ignition delays. Laminar flames were simulated using PREMIX in CHEMKIN PRO with values GRAD and CURV parameters set to 0.02 and 0.03, respectively, which resulted in grid independent solutions for all mechanisms. Due to convergence difficulties in CHEMKIN the Cantera software v. 2.3.0 [80] was used for the simulation of the laminar burning velocities for the global mechanisms (WD1, WD2, and JL4). There an adaptive grid refinement was used, resulting in a grid with roughly 500 grid points.

Ignition was modelled with SENKIN in CHEMKIN PRO using a constant volume approach. Sensitivity analysis of ignition delay was performed with a brute-force approach using the program Igdelay [81].

An important consideration when simulating flames is the representation of transport. In the present work the mixture-averaged approach (MIX) was used to determine species diffusion coefficients and fluxes. A more time-consuming approach is to use a multicomponent (MULT) formulation. In addition, a thermal diffusion coefficient, called the Soret effect, can be included, considered important for light species like H_2. These more detailed treatments are standard for use in detailed modeling of 0D/1D systems for research purposes. Technical details on the different approaches we refer the reader to the manual for CHEMKIN PRO [79]. However, in CFD simulations the limitations in computational capacity require use of the mixture-averaged treatment of transport and therefore it is relevant to evaluate the mechanisms using this approach. One should keep in mind that transport treatment becomes increasingly important as size of species decrease and therefore larger deviations can be expected for hydrogen flames. Figure A1 in Appendix A present laminar burning velocities for methane/air flames at standard conditions for two mechanisms evaluated in the present study, the detailed GRI-Mech 3.0 and the reduced Z42 mechanism, with different transport treatment. The simple MIX approach gives higher laminar burning velocities with a few cm/s, in particular at peak conditions. This is, however, in the present circumstances not considered as significant deviations.

5. Mechanism Evaluation

In this section the mechanisms are evaluated by comparison to experimental data for the important combustion characteristics, where available. Validation targets are selected among reliable literature data to cover a range of properties (ignition, propagation, extinction, speciation) and conditions (T, P, ϕ), for which experimental data are available. All cases have been simulated with the mechanisms Aramco, SD, GRI, USCII, Z42/45, SG35, SR35/39 and DRM22, if nothing else stated. Validation targets are summarized in Table 5. In the figures each mechanism is represented by lines according to caption in Figure 1, if nothing else is stated.

The mechanism evaluation starts with regular methane/air combustion, which is the fuel/oxidizer mechanism that the mechanisms have been constructed to predict. This is followed by considerations about the performance as other species are included.

Table 5. Experimental validation data used in the present review.

Property	Type	Fuel	P (atm)	T (K)	ϕ	Ref
S_L	Heat flux method	CH_4 CH_4/H_2	1–5	298	0.8–1.4	[10,36,46,82]
S_L	Counter flow		1, 5, 10	298, 360, 400		[83]
S_L	Spherical flame	CH_4 CH_4/H_2	1, 5, 10	298, 443	0.7–1.3	[43–45,47]
S_L	Bunsen flame			343–523	0.6–1.3	[84]
t_{ig}	Shock tube	CH_4	1–115	1100–2000	0.1–3.0	[47,85,86]
t_{ig}	Shock tube	CH_4/H_2	16–40	1000–1550	0.5–1.0	[87,88]
[CH]	Stagnation flame	CH_4	1	296	0.7–1.3	[89]
σ_{ext}	Counter flow flame	CH_4	1	298	0.7–1.0	[83]
Species profiles	Perfectly stirred reactor	CH_4 CH_4/H_2	10		0.3	[90]

5.1. CH_4/Air Combustion

5.1.1. Ignition Delay Time CH_4/Air

Ignition delay time at pressures up to 115 atm and from the lean combustion limit and up to very rich equivalence ratios were investigated, see Table 5. In this subsection the trends are summarized and exemplified with a few figures. Additional figures are included in Appendix A.

In Figure 2 the experimental data and modeling using detailed and reduced mechanisms are presented for stoichiometric flames at 1 atm. Figure 4 presents modeling and experimental data for lean and rich fuel mixtures and at elevated pressure, with experimental data from Hu et al. [47] and Petersen et al. [85].

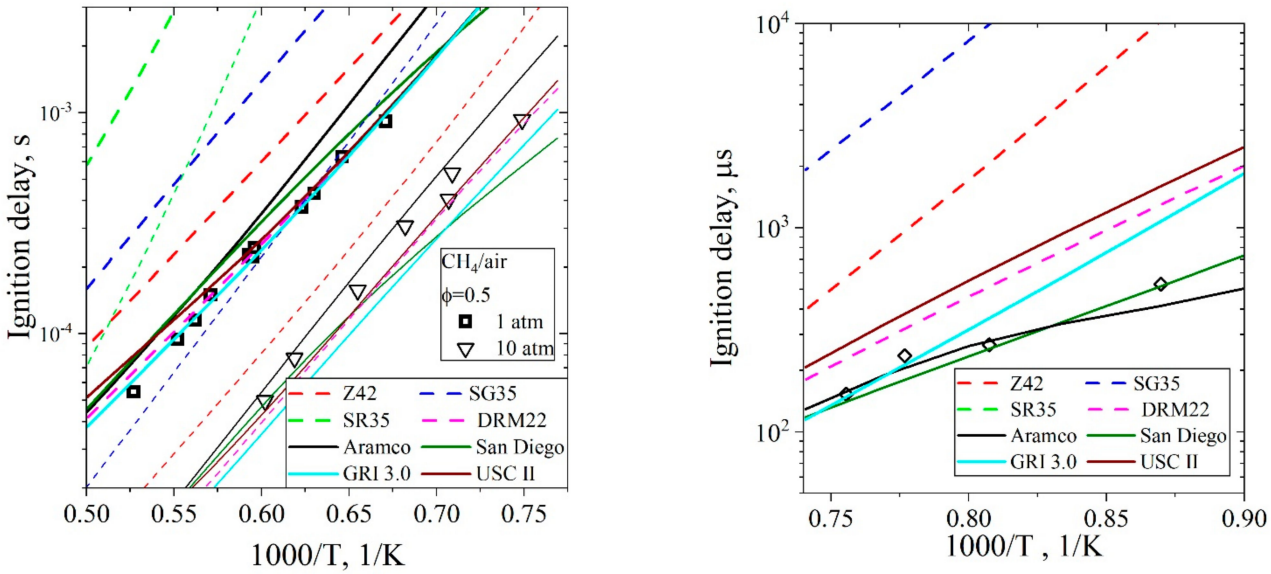

(**a**) (**b**)

Figure 4. Shock tube ignition delay times. (**a**) lean conditions in the temperature range 1300–2000 K and at pressures of 1 and 10 atm. (**b**) for rich conditions of ϕ = 3.0 in the temperature range 1100–1550 K at pressure 115 atm. Lines are modelling predictions by detailed and reduced mechanisms (in (**a**) narrow lines: 10 atm, thicker lines: 1 atm) and symbols experimental data by Hu et al. [47] and Petersen et al. [85].

In general, the detailed mechanisms are in good agreement with experimental data. The reduced mechanism predicts longer ignition delay times, for SR35 by more than an order of magnitude. The inclusion of additional reactions to give the SR39 mechanism was tested for the studied range of conditions and it did not result in any improvements

compared to SR35. Z42 predict higher reactivity (shorter ignition delay time) than its mother mechanism SG35, which indicate that the modifications are valid, but it still does not accurately reproduce the experimental data. To further understand the difference between the reduced mechanisms a sensitivity analysis was performed (Figures in Appendix A). From the analysis it is clear that the slower reacting SR35 mechanism among its most sensitive reactions have a large proportion of slow reactions of hydrocarbon fragments, while the more reactive mechanisms to a larger extent rely on the small radicals' chemistry.

The good agreement of DRM22 with the detailed mechanisms indicate that a mechanism of this size, a few more species and more than the double number of reactions compared to the other reduced mechanisms, can give a truly versatile compact mechanism.

At the highest pressures the spread in mechanism predictions is large, with the reduced mechanisms doing worse than at the lower pressures. Unfortunately, the high-pressure chemistry is not well understood and the implementation also in the detailed mechanisms may not be accurate, as evident from the more than order of magnitude differences between detailed mechanisms seen in Figure 4b.

5.1.2. Laminar Flames of CH_4/Air

Laminar flames at standard conditions, initial gas mixture temperature of 298 K and at a pressure of 1 atm (Figure 1), have been studied extensively using various experimental methods and is the first target for most kinetic mechanisms. The scatter in results from experimental studies shown in Figure 1 can be considered as an indication on how well the property S_L is known. The recent and highly detailed mechanism from NUI Galway, Aramco Mech, is considered as the benchmark since it builds on most recent reaction rate constants and is validated towards extensive datasets. The differences between the different mechanisms presented in Figure 1 can be further analyzed from the representation in Figure 5 where deviation in laminar burning velocity for each mechanism compared to the benchmark, in percent, is plotted. The detailed kinetic mechanisms, represented by solid lines, are in satisfactory agreement with experimental results (see Figure 1), with quite good agreement at lean conditions and larger scatter in experimental results and between the mechanisms at rich conditions. Figure 5 reveals interesting trends in how laminar burning velocity predicted by reduced and global mechanisms deviate from the benchmark detailed mechanism, with commonly 20–25% over prediction at lean conditions and for the reduced mechanisms under predictions overlarge part of stoichiometric and rich conditions. It is clear from both Figures 1 and 5 that the global mechanisms significantly fail at rich conditions. Flame temperature profiles, Figure 1b, are essentially identical up to equivalence ratio of about 1.4, except for SR35. At the richest conditions also the two reduced mechanism of about the same size, SG35 and Z42, show too high flame temperatures.

Sensitivity analysis, Figure 6, reveals that that the reduced mechanism Z42 share the most important reactions with the detailed Aramco mechanism. A significant difference is that the detailed mechanism includes C2 chemistry that becomes important at rich conditions, in particular those reacting with hydrogen atom. A reduced mechanism suitable for use in most CFD simulations will become too large if the C2 chemistry is incorporated, and to compensate for this the C1 reactions are given a more significant role, including reactions of CH and CH_2 for the Z42 mechanism. In general, the reduced mechanism has similar chemistry as the detailed mechanisms at lean conditions.

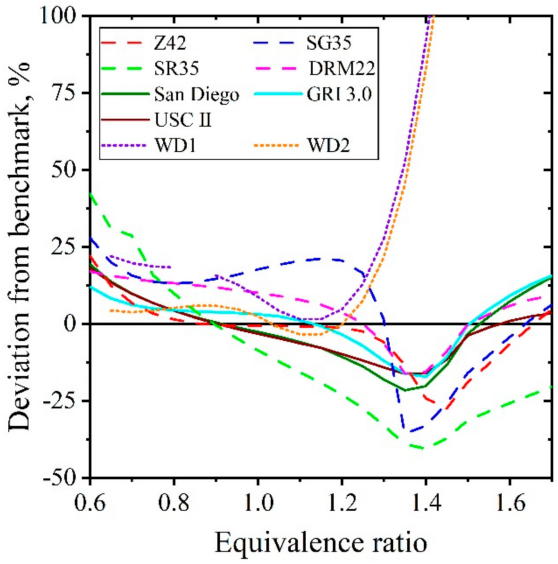

Figure 5. Percentage deviation in laminar burning velocity compared to the benchmark mechanism (Aramco Mech) for the mechanisms presented in Figure 1.

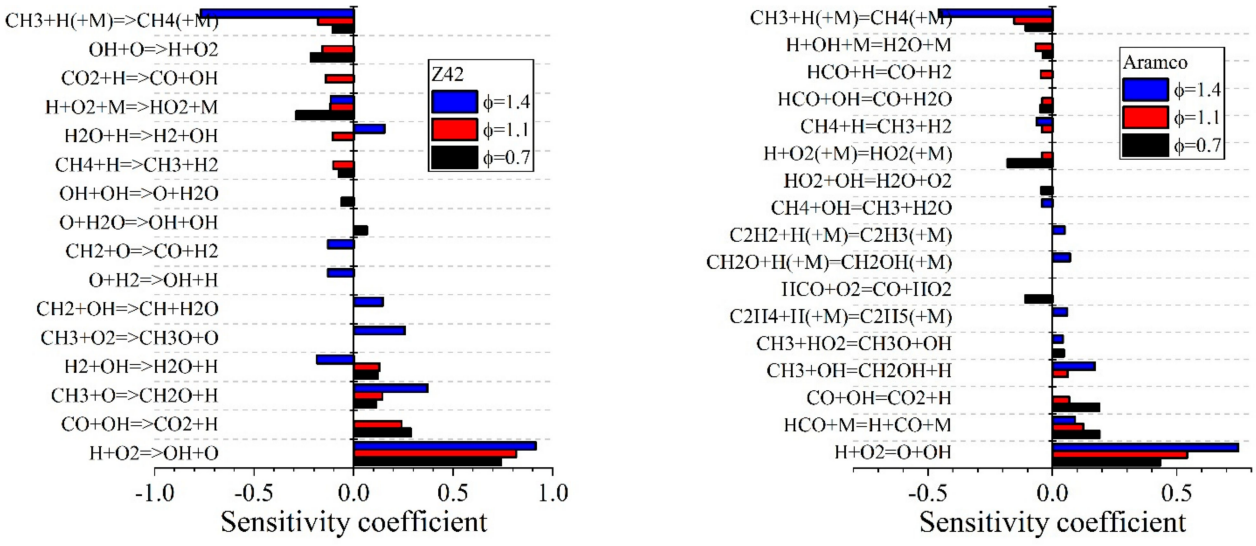

(**a**) (**b**)

Figure 6. Sensitivity coefficients for the ten most sensitive reactions for the reduced mechanism Z42 (**a**) and the detailed Aramco Mech 2.0 (**b**), at standard conditions of 298 K and 1 atm.

Figures 7 and 8 present laminar burning velocities at elevated pressures and temperatures. The overall behavior for the mechanisms with increasing temperature and at 1 atm pressure, Figure 7a, is similar to that at ambient conditions, while the increase in pressure is handled differently between the mechanisms with change of the overall shape of the curve, as evident in Figure 8a. In case of the reduced mechanisms Z42 is the only one which retains its curve shape whereas SG35, SR35, and DRM22 all have a tendency for a shift of the curve towards the lower equivalence ratios, as pressure increase. The trend in laminar burning velocity for increasing gas mixture temperatures are shown for a rich case in Figure 7b, where SG35 and SR35 show deviations from the other mechanisms.

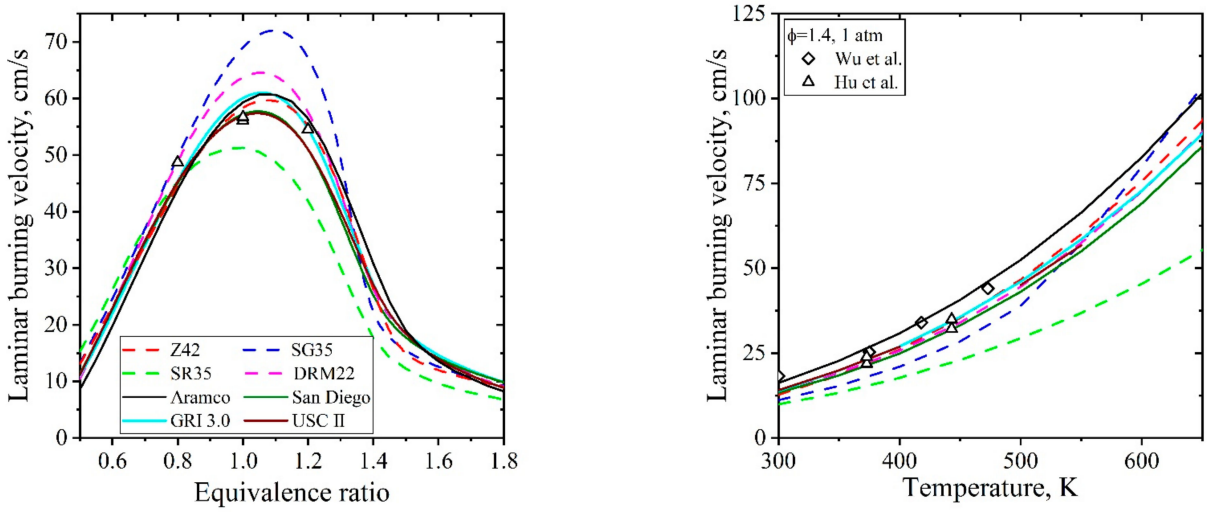

(**a**) (**b**)

Figure 7. Laminar burning velocity of CH_4/air flame at (**a**) 400 K and 1 atm, and (**b**) as function of initial gas mixture temperature for rich (ϕ = 1.4) conditions. Experimental data [43,47,84] represented by symbols, and modeling by lines.

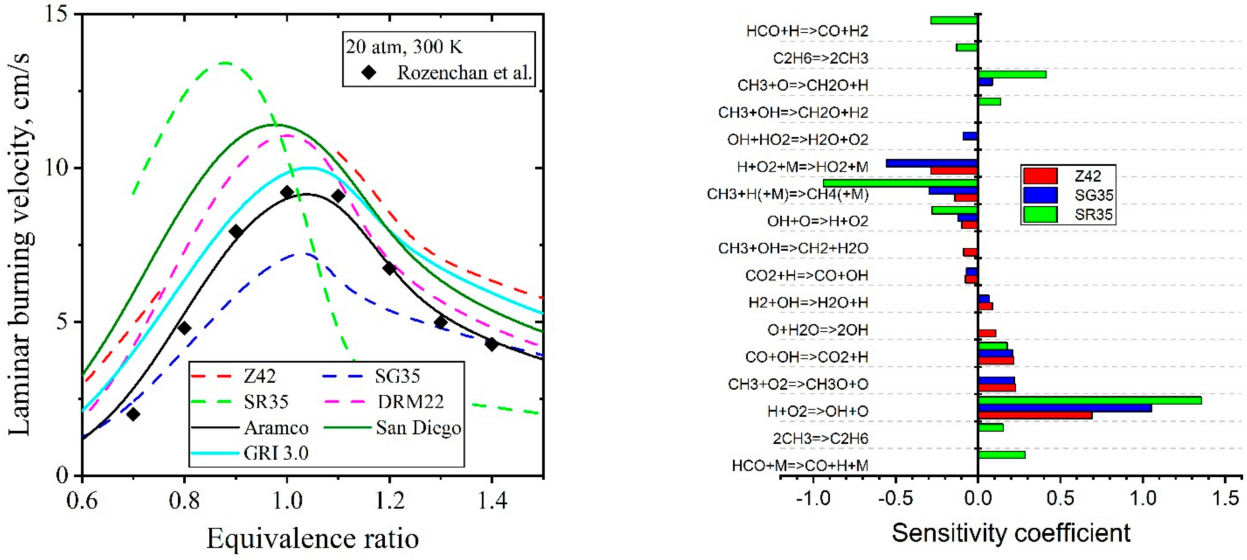

(**a**) (**b**)

Figure 8. Laminar burning velocity of CH_4/air flame at (**a**) 300 K and 20 atm (**b**) sensitivity coefficients for the three reduced mechanisms Z42, SG35 and SR35 at ϕ = 1.0, 300 K and 20 atm. Experimental data [36,43–45,83], represented by symbols.

Figure 8a show laminar burning velocities at pressure 20 atm. One should note that the laminar burning velocities at higher pressure is much lower and that the absolute difference between the mechanisms is about the same as for the lower pressure, 1–5 cm/s. At the higher pressure conditions, the trend among the detailed mechanisms are still that they give similar results, except that the skeletal DRM22 deviates more than it did at ambient pressure. It is worth to note that the SG35 mechanism under predict laminar burning velocity at high pressure, while it made over predictions close to ambient pressures. There is clearly a mistreatment of pressure dependence in this mechanism and it cannot be recommended for use in simulations at elevated or varying pressure. The difference in treatment of pressure in the three reduced mechanisms, Z42, SG35, and SR35, are shown in the sensitivity analysis in Figure 8b. Here SR35 shows a quite different pattern, with several C2 reactions among the most sensitive.

Trends in laminar burning velocity with increasing pressure up to 30 atm are presented in Appendix A. As seen in many of the figures earlier, the agreement between mechanisms are better at lean conditions. Figure 9 shows deviation of three reduced mechanisms from the benchmark for laminar burning velocity simulations at elevated pressure of 10 atm. At leanest and richest conditions where absolute values of laminar burning velocity are low, it is apparent that the deviation from the benchmark is commonly larger.

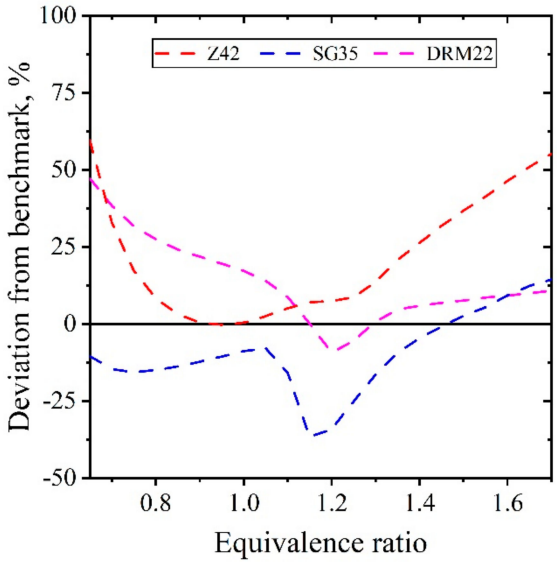

Figure 9. Deviation from the benchmark mechanism (Aramco Mech) for the reduced mechanisms DRM22, Z42, and SG35. Results for simulations of laminar burning velocity at initial gas mixture temperature of 300 K and pressure of 10 atm.

Concentration of CH has not been used as a target in development of any of the mechanisms, neither the detailed nor the reduced. CH can, however, be quite important since it is used as an indicator for ignition in experimental studies, and therefore the modeling studies need to accurately predict its production, at least the onset of CH production. A second motivation for accurate prediction of CH is its importance in the chemistry of hydrocarbon combustion in electric fields, so-called plasma assisted combustion. Among the reduced mechanisms evaluated here only Z42 include CH. Experimental data on CH concentration in methane flames is scarce, but Figure 13a present experimental estimations produced by Versailles et al. [89], together with modeling predictions. Peak mole fractions at $\phi = 1.2$ are scattered in the range of about 1 to 10 ppm, with the experimental estimate at about 4 ppm. One of the detailed mechanisms, San Diego, is in good agreement with the experiments, but whether this depends on more accurate treatment of relevant chemistry cannot be concluded from the present study. Figure 13b present profiles of CH as a function of height above the burner, and it can be seen that the mechanisms give slightly different position of the CH layer in these flames.

5.1.3. Extinction Strain Rate of Premixed CH_4/Air Flames

Extinction has not been studied extensively in laboratory setups, here we rely on a single publication by Park et al. [83]. The lack of data and on the attention on these phenomena result in that reduced mechanisms are seldom constructed to accurately prediction extinction. Figure 10 presents extinction strain rate at standard conditions for lean equivalence ratios in Figure 10a. The detailed mechanisms represent the experimental data fairly well, while the reduced mechanisms show an increasing deviation at closer to stoichiometry. In Figure 10b, the development of the extinction strain rate with temperature is pictured for two equivalence ratios and it is seen that the reduced mechanisms make very different predictions, but that they have in common that they predict extinction at

lower temperatures than the detailed mechanisms. For the use of the reduced mechanisms in CFD this mean that the flames are likely to extinct prematurely.

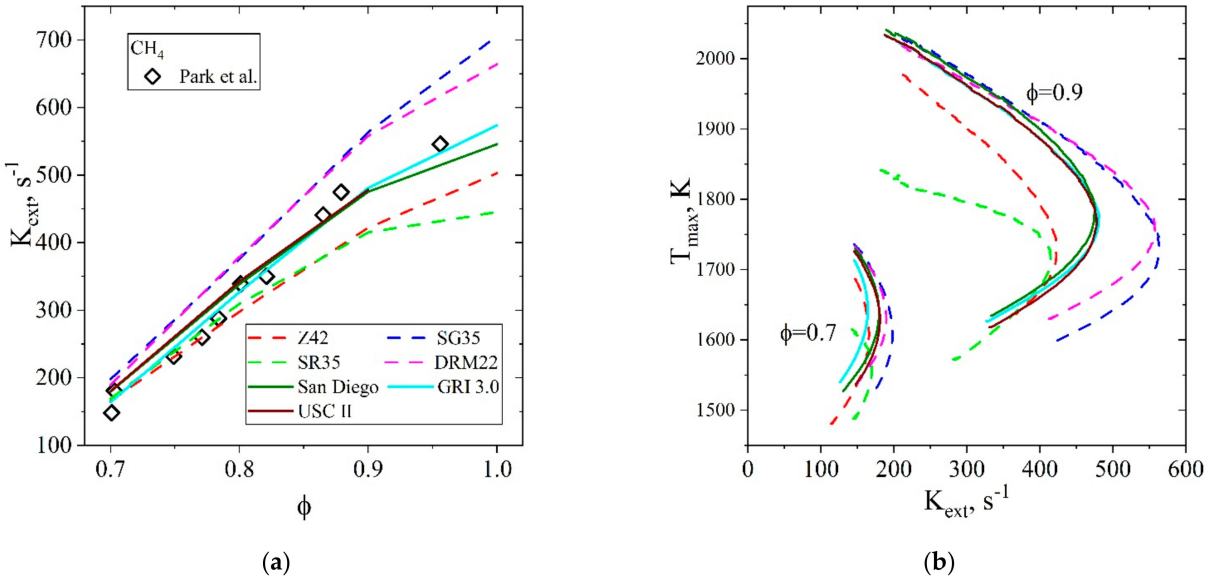

(**a**) (**b**)

Figure 10. Extinction strain rate (**a**) as a function of equivalence ratio for methane/air mixture counter flowing with a N_2 jet, at standard conditions of 298 K and 1 atm [83], (**b**) the development of the strain rate with temperature.

5.2. Flames at CO_2 Enriched Conditions

Figure 11 presents laminar burning velocities for a combustible mixture consisting of CH_4 and CO_2, at pressures 1 and 4 atm and an initial gas temperature of 300 K. A majority of CO_2 is formed from a small set of reactions making the sub mechanism for CO_2 limited in size. All mechanisms reviewed here contain the most important reactions in that sub mechanism, so the predicted laminar burning velocities shown are similar, regardless of mechanism size. Especially the detailed mechanisms, which contains highly similar CO/CO_2 chemistries, the same burning velocities are more or less predicted regardless of pressure.

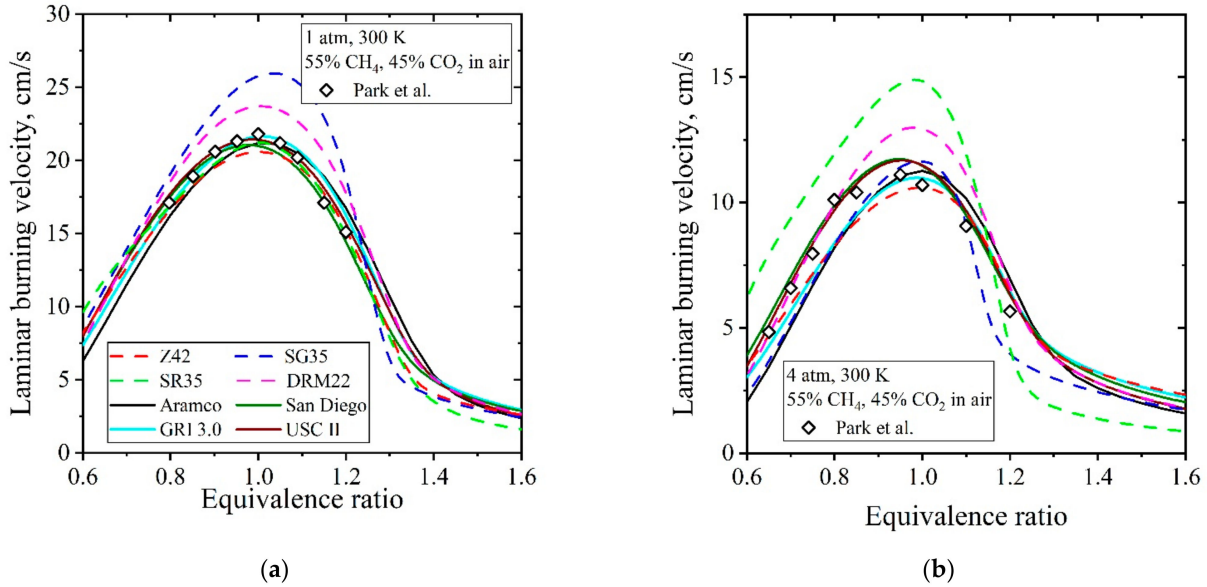

(**a**) (**b**)

Figure 11. Laminar burning velocity of CH_4(55%)/CO_2(45%)/air flames at (**a**) 1 atm and (**b**) 4 atm at initial gas mixture temperature of 300 K. Experimental data [83], represented by symbols, and modeling represented by lines.

The previously mentioned CH_2/CH subset of Z42 compared to SG35, together with updated rates for the conversion of CO_2 back to CO, is enough to extensively improve the results for Z42 compared to SG35 when additional CO_2 is added to the mixture. This shows how small changes in a mechanism can profoundly broaden the applicability of a mechanism as well as improving its results.

5.3. CH_4/H_2/Air Combustion

5.3.1. Ignition Delay Time CH_4/H_2/Air

Addition of hydrogen to methane increase the reactivity of the system and thus shorten the ignition delay time. It has been shown in previous modelling works that at the moderate levels of H_2 (below 40%) considered here the chemistry is very much the same as for methane ignition, but with a larger radical pool of particularly H that increase the reactivity of the system via reaction with O_2.

Figure 12 presents ignition delay times for H_2 in CH_4 and it is clear that the reduced mechanisms diverge strongly from experimental data and detailed mechanisms at the lower temperatures. Regarding the Z42/Z45 mechanisms they give about the same results for the highest temperatures, while Z45 is in significantly better agreement at the low temperatures. The low temperature ignition for these experiments have been shown to be dominated by CH_3O_2 chemistry, reaction subsets that are not available in any of the reduced mechanisms. Z45 does, however, compensate for this by the additional H-producing reactions that increase the overall reactivity to make accurate predictions of ignition delay time.

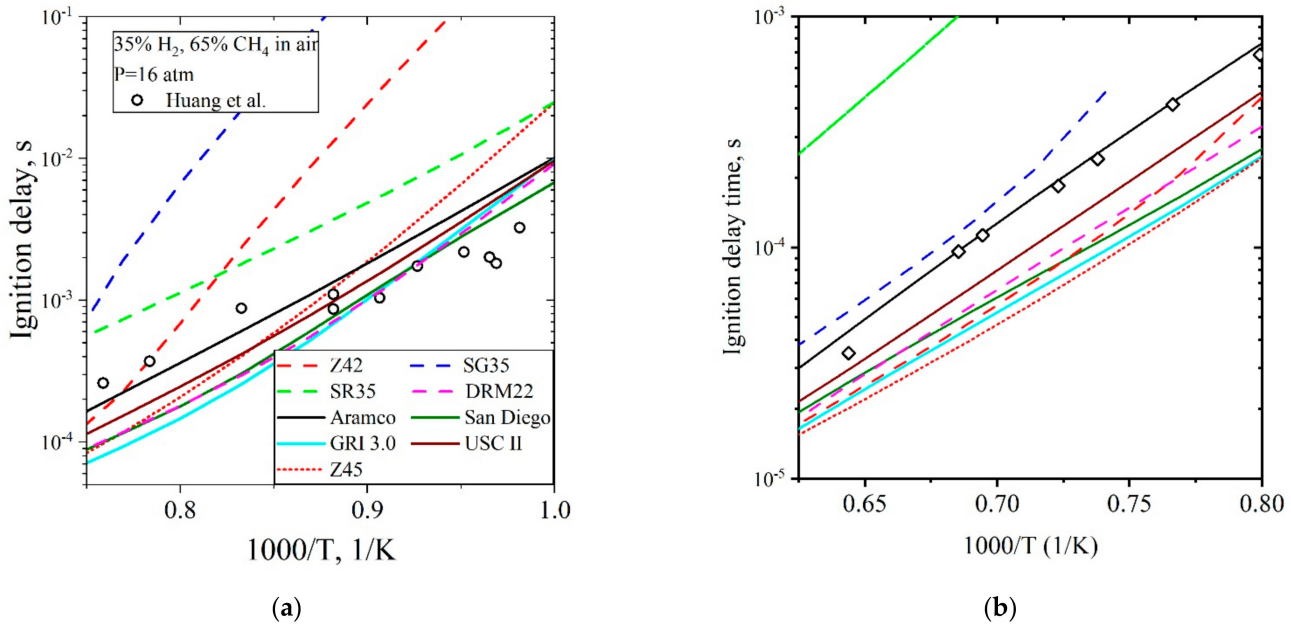

Figure 12. Ignition delay for (**a**) stoichiometric mixtures with 35% H_2 and 65% CH_4 in air at 16 atm and (**b**) lean (ϕ = 0.5) mixtures with 20% H_2 and 80% CH_4 in air at 20 atm. Experimental data from Huang et al. [88] and Petersen et al. [87]. Short dotted red line is Z45.

5.3.2. Laminar Burning Velocity CH_4/H_2/Air

At a moderate hydrogen enrichment of 50%, Figure 14a, the trends for different mechanisms are similar to that of the conditions without any hydrogen, Figure 1. All detailed mechanisms and Z42 show similar predictions, with SG35 as for pure CH_4/air mixtures over predicting the burning velocity around stoichiometric conditions and SR35 fail to provide a solution. The Z45 mechanism with reactions for hydrogen decomposition added to Z42 showed identical performance as Z42 for flames.

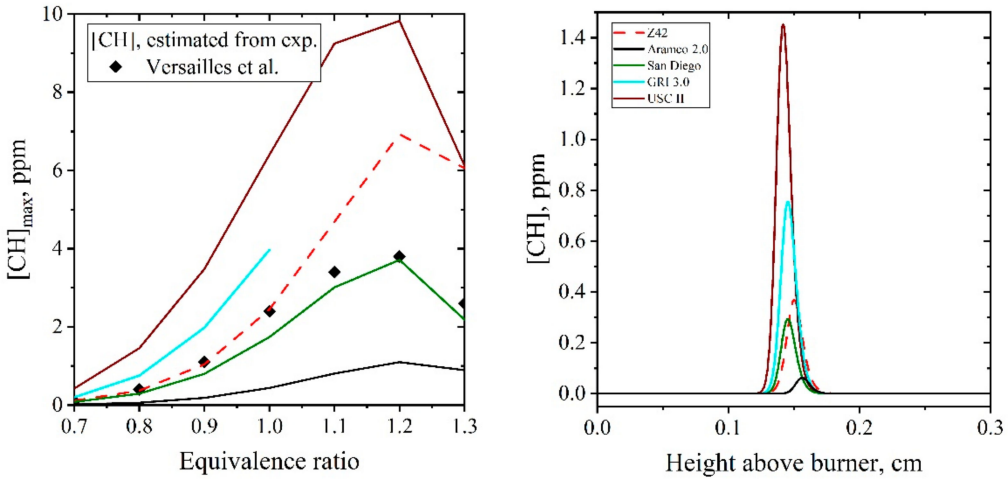

(**a**) (**b**)

Figure 13. (**a**) Maximum mole fractions of CH in premixed laminar flames at 296 K and 1 atm, symbols represent experimental estimates [89] and lines modeling. (**b**) profiles of CH as a function of height above the burner at ϕ = 0.8. SG35, SR35, and DRM22 are not presented since they do not include CH.

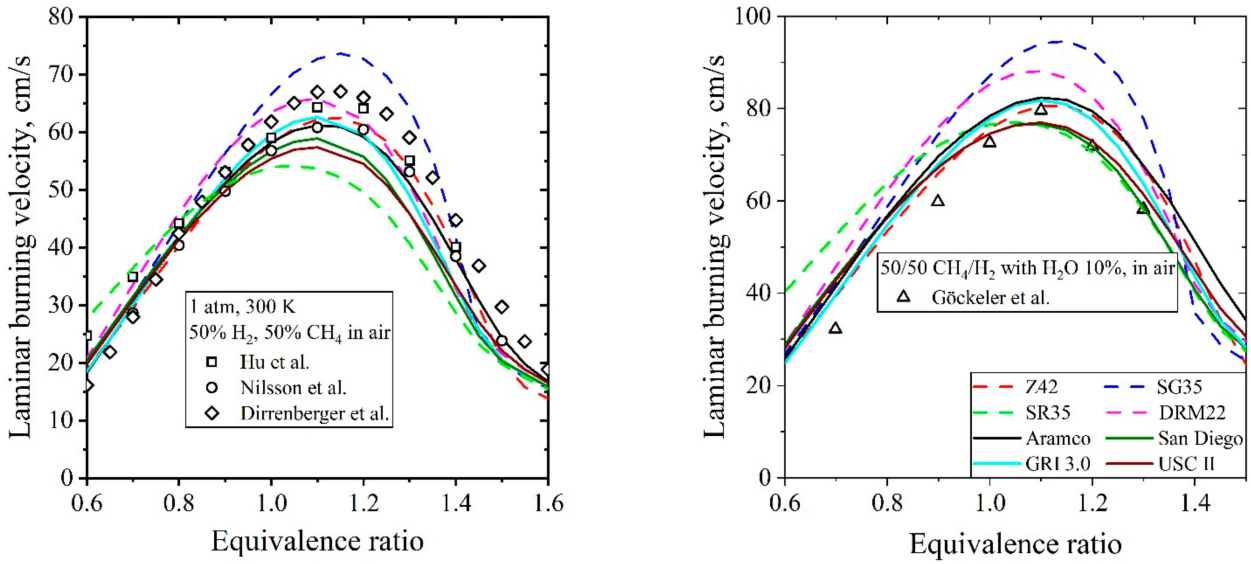

(**a**) (**b**)

Figure 14. Laminar burning velocity for (**a**) methane/hydrogen/air flames with 50% H_2 at 300 K and pressure 1 atm and (**b**) methane/hydrogen/water/air flames with 10% water at 440 K and pressure 1 atm. Experimental data [33–36,91], represented by symbols, and modeling [7,9–11,16,30] represented by lines.

As water is also added to the system, Figure 14b, the performance is similar as without water, which mean that the mechanisms have the ability to handle some water addition.

Figure 15 presents laminar burning velocities as a function of hydrogen fraction, for lean and rich conditions, and from this figure it is apparent that all mechanisms are in fairly good agreement and reproduce the experimental trends within the spread between data points.

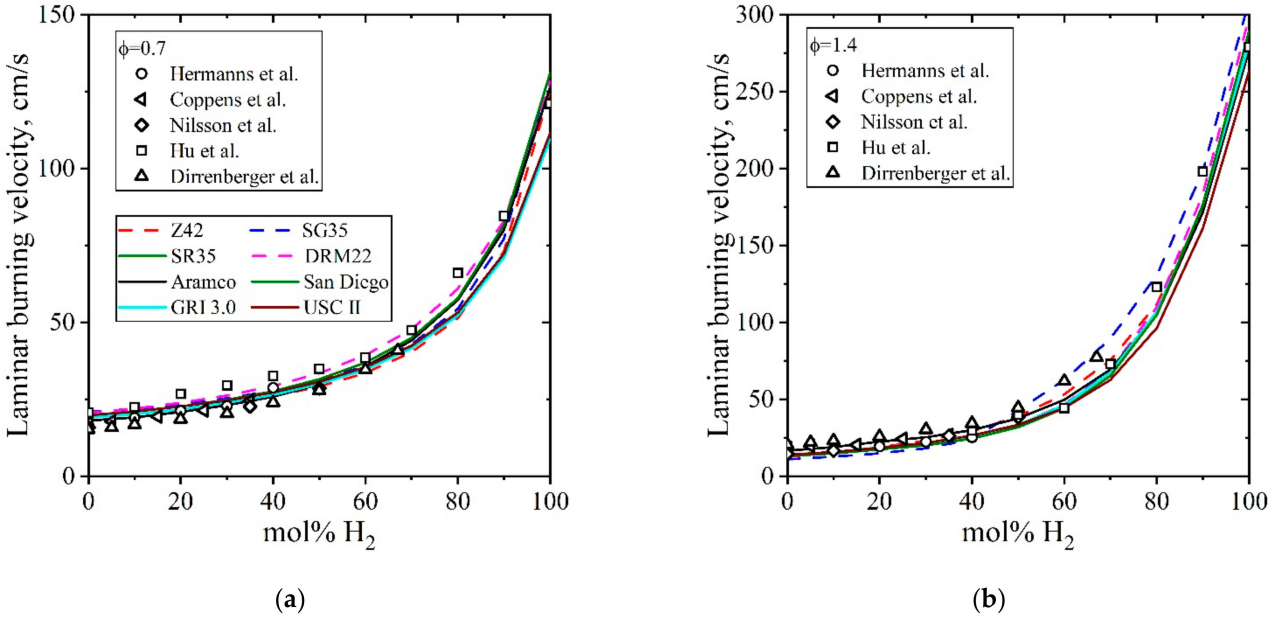

(**a**) (**b**)

Figure 15. Laminar burning velocity for methane/hydrogen/air flames as a function of H_2 fraction in the fuel at equivalence ratios (**a**) ϕ = 0.7, and (**b**) ϕ = 1.4. Initial gas mixture temperatures of 300 K and pressure 1 atm. Experimental data [30–33], represented by symbols, and modeling [7,9–11,16,30] represented by lines.

5.4. Syngas, CO/H_2/Air, Flames

Syngas, being composed of a mix of CO and H_2, relies heavily on both the CO/CO_2 chemistry important for the CH_4/CO_2/air mixtures and the H_2/O_2 chemistry important for the CH_4/H_2/air mixtures. In Figure 16 flame modeling of syngas flame is presented, to investigate the comprehensiveness of the mechanisms. The detailed mechanisms hold an advantage to the smaller ones when it comes to syngas combustion due to the higher number of initiation reactions present, often including reactions for both CO and H_2. This is not something that smaller mechanisms can afford, due to the minimalistic nature of such mechanisms in order to reduce the computational cost.

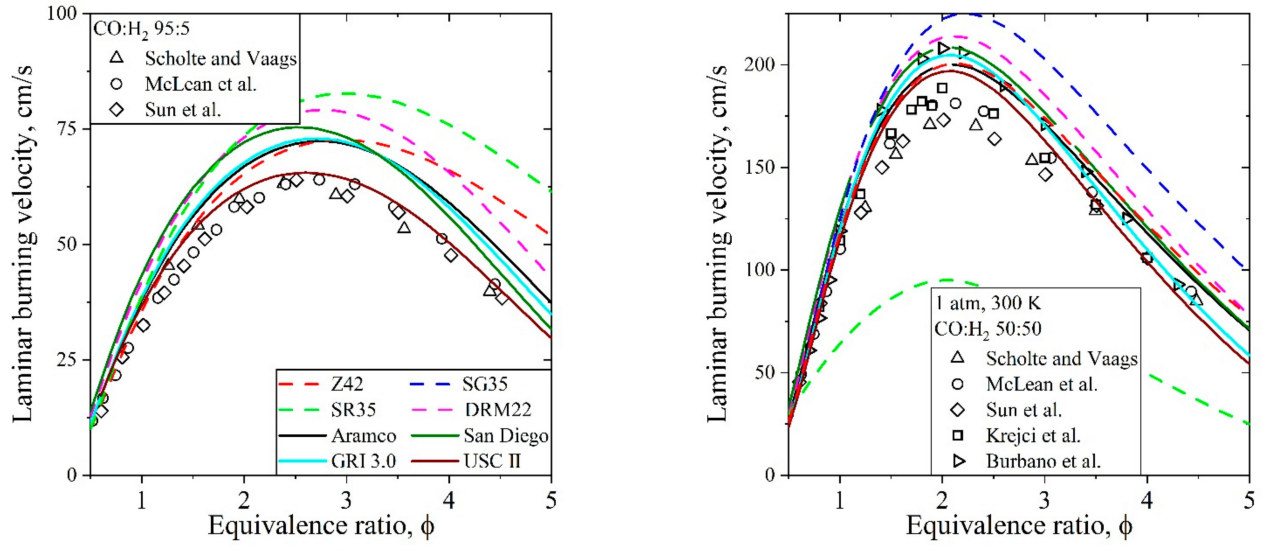

(**a**) (**b**)

Figure 16. Laminar burning velocity for syngas mixtures with composition CO:H_2 of 95:5 (**a**) and 50:50 (**b**) at 1 atm and 300 K. Experimental data presented by symbols [92–96].

The close match between Z45 and the experimental data may come as a surprise due to the lack of initiation reactions for CO and to the simple nature of the CO/CO_2 chemistry in Z45. Z45 relies entirely on the initiation of H_2 in order to start the combustion process, and even in cases with only 5% H_2 Z45 still achieves well predicted burning velocities.

6. Discussion and Recommendations

6.1. Detailed Mechanisms

The detailed mechanisms have, as referenced in the early sections of this work, been evaluated elsewhere but there are some important comments to make about the mechanisms in relation to CFD and reduced mechanism development. Aramco Mech, San Diego, and USC II have in common that they are regularly updated as a response to new experimental evidence. This is not true for the GRI 3.0 Mech, and the use of this mechanism outside conditions for which it was initially validated for is not recommended.

The mechanism with best overall performance is the Aramco Mech which accurately reproduces all validation data in this work, except the CH concentration in flames. We recommend the use of Aramco Mech as benchmark in 0D/1D simulations, in particular when there is a significant interest in ignition. Regarding time consumption Aramco Mech is by far the slowest mechanism, requiring tens of minutes and up to hours to calculate laminar burning velocity at one set of conditions. This can be compared to GRI 3.0 which uses about one minute for the same simulation. The San Diego and USC II mechanisms are in fairly good agreement with Aramco Mech over a wide range of conditions and are significantly smaller and faster than Aramco Mech, which motivates their use when a detailed mechanism is needed but computational capacity is limited. Regarding time consumption, the USC II mechanism simulates a laminar flame in about ten times the time as GRI 3.0, while the San Diego mechanism is in between the two.

All the mentioned detailed mechanisms are used as starting points for mechanism reduction using automated reduction methods. From a point of view of comprehensiveness and accuracy of chemistry the Aramco Mech should be most suitable for mechanism reduction. However, considering the size of the mechanism it may be too time consuming. The GRI 3.0 is not suitable for automated mechanism reduction since it in itself does not include the most accurate chemistry, if a smaller detailed mechanism is needed for mechanism reduction it is more advisable to use San Diego or the USC II mechanism.

6.2. Reduced Mechanisms

For the three reduced mechanisms of similar size, SR35, SG35, and Z42, the simulation takes about 5% of the time for the GRI 3.0 mechanism to perform the corresponding simulations. To present the numbers: when GRI 3.0 use 1 min the reduced mechanisms need only in the range 2–4 s. The fastest mechanism is SG35, while SR35 and Z42 take about the same time. All of them are faster simulating flames at lean conditions (2–4 s) compared to rich conditions (4–8 s), which is an indication of the more complex chemistry at the rich conditions.

If the simulation targets are flames at lean conditions, below about $\phi = 0.8$, all the reduced mechanisms will give about the same results for flame propagation, heat release, and major species concentrations. Even though the computational time is very short for all of them, SG35 is the winner in a case where small reduction in computational time is a significant advantage. For other cases we would like to recommend the Z42 mechanism since it is useful over a wide range of flame conditions, and also performs best for ignition delay time. Z42 is also the reduced mechanism that has reactions in best agreement with the detailed mechanisms, as shown using sensitivity analysis. The reduced mechanism that we cannot recommend for use is the SR35, it show overall least agreement with experiments and detailed mechanisms, and it appeared to miss some of the important high pressure chemistry.

All three highly reduced mechanisms have too low reactivity for ignition, resulting in too long ignition delay times. The DRM22 with its 104 reactions does a much better job for

ignition, indicating the need to include more reactions, but that a quite small mechanism is still possible.

The addition of H_2, CO_2, and H_2O is handled almost as accurately as pure methane for SG35 and Z42, while SR35 also in these cases is inferior. Based on this we could recommend the use of Z42 for various mixtures of relevance for example in simulation of gas turbine combustion. Additionally, SG35 would perform fairly well at lean conditions.

6.3. Global Mechanisms

Regarding global mechanisms, it is necessary to use them only for conditions that they are parameterized for, and not where accurate ignition or extinction events need to be modelled. While the early mechanisms by Westbrook and Dryer and Jones and Lindstedt include reactions that are of relevance to any global mechanisms, we cannot advise using their original parameterization outside the very specific range of conditions that they are valid for. The more recent global mechanisms use better parameterization and should be preferred.

Global mechanisms have the advantage that there are few species and reactions, but sometimes they unfortunately have a considerable stiffness. The experience from running the simulations in CHEMKIN and Cantera is that there are often convergence problems with global mechanisms and the computational time is actually close to that for the reduced mechanisms of around forty reactions.

6.4. Summary and Outlook

Regarding all detailed mechanisms, it is advisable to use them for mechanism reduction only within the parameter space they have been validated in. However, we are very well aware that reduced mechanisms often are needed at conditions for which no detailed mechanism has been evaluated. The present work has investigated the common detailed mechanisms over a wider parameter range than they were originally constructed for and the results can be used as a guide in selection of detailed mechanism for automated reduction.

For CFD, where the DRM22 mechanism with its 22 species and 104 reactions can be afforded, we recommend its use since it is in good agreement with the benchmark over a wide range of conditions for both flames and ignition. When a smaller mechanism is needed, the Z42 with only 42 irreversible reactions is highly recommended. For flame propagation Z42 is as good as DRM22, while the larger mechanism is more accurate in predictions of ignition.

Author Contributions: Conceptualization, C.F. and E.J.K.N.; validation, E.J.K.N.; formal analysis, E.J.K.N.; investigation, N.Z. and E.J.K.N.; resources, E.J.K.N.; writing—original draft preparation, E.J.K.N.; writing—review and editing, C.F., N.Z., E.J.K.N.; visualization, E.J.K.N. All authors have read and agreed to the published version of the manuscript.

Funding: This research was funded by the Swedish Energy Agency.

Institutional Review Board Statement: Not applicable.

Informed Consent Statement: Not applicable.

Data Availability Statement: Not applicable.

Acknowledgments: The authors gratefully acknowledge the financial support from the Swedish Energy Agency through the Centre of Combustion Science and Technology (CECOST).

Conflicts of Interest: The authors declare no conflict of interest.

Appendix A

Appendix A present Figures A1–A8 illustrating the performance of the mechanisms, discussed in the main text.

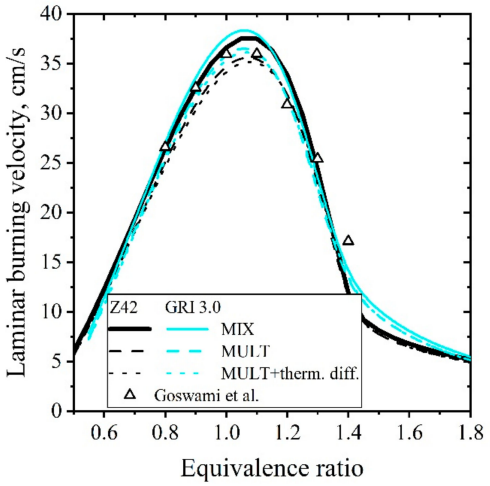

Figure A1. Laminar burning velocities of methane/air flames at 298 K and 1 atm, with experimental data from Goswami et al. [36]. Modeling with GRI 3.0 and Z42 using different approaches to transport.

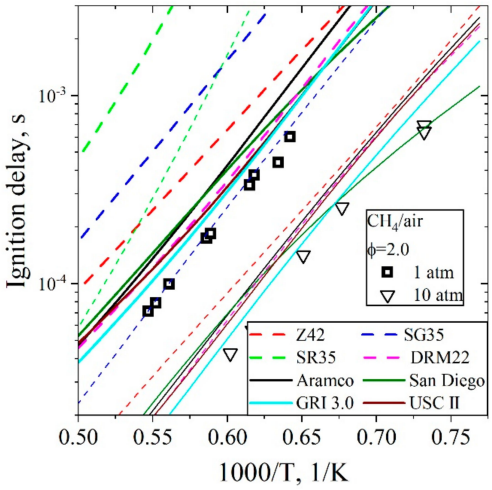

Figure A2. Shock tube ignition delay times over the temperature range 1300–2000 K at pressures of 1 and 10 atm, for rich conditions. Lines are modelling predictions by detailed and reduced mechanisms (narrow lines: 10 atm, thicker lines: 1 atm) and symbols experimental data by Hu et al. [47].

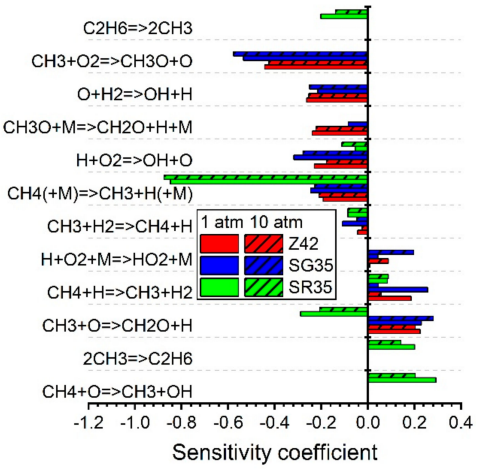

Figure A3. Sensitivity coefficients for ignition delay for the three reduced mechanisms Z42, SG35 and SR35 at stoichiometric conditions. Temperature 1500 K and pressure 1 and 10 atm.

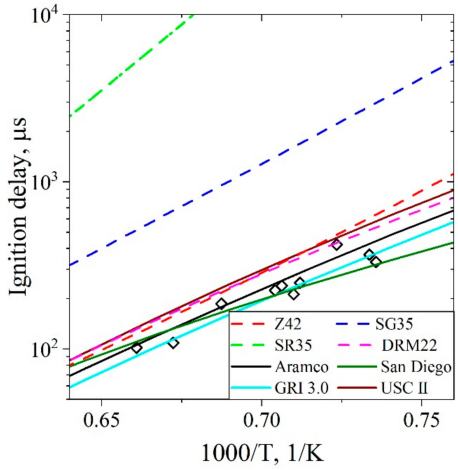

Figure A4. Shock tube ignition delay times over the temperature range 1100–1550 K at pressures of 40 atm for rich conditions of ϕ = 3.0. Lines are modelling predictions and symbols experimental data by Petersen et al. [85].

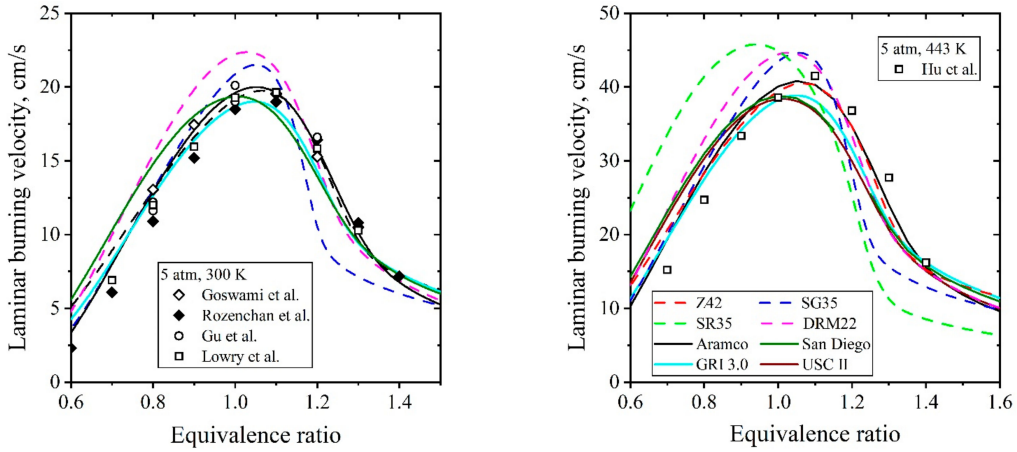

(**a**) (**b**)

Figure A5. Laminar burning velocity of CH_4/air flame at (**a**) 300 K and 5 atm and (**b**) 443 K and 5 atm. Experimental data [36,43–45,83] represented by symbols, and modeling by lines.

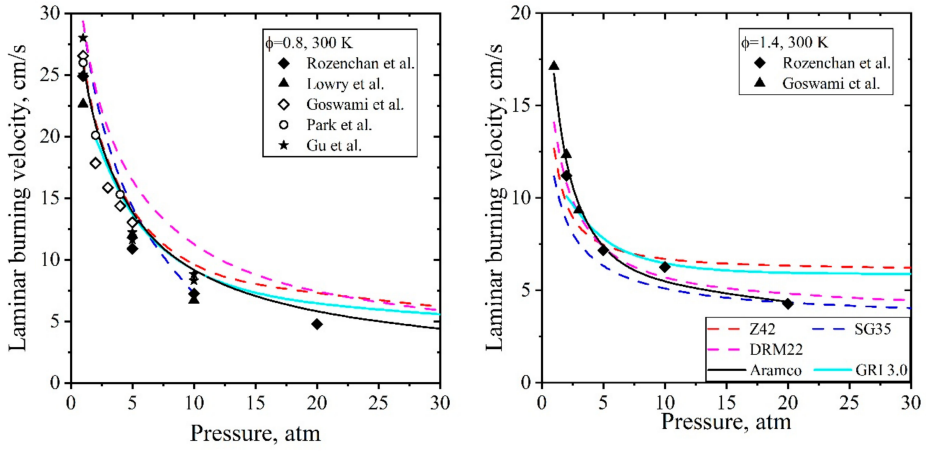

(**a**) (**b**)

Figure A6. Laminar burning velocity of CH_4/air flame as function of pressure at (**a**) ϕ = 0.8, and (**b**) ϕ = 1.4. Experimental data [36,43–45,83] represented by symbols, and modeling represented by lines.

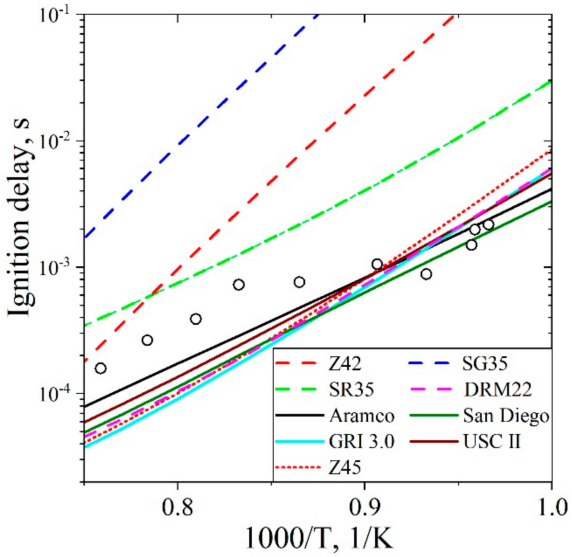

Figure A7. Igniton delay for stoichiometric mixtures with 35% H_2 and 65% CH_4 in air at 40 atm. Experimental data from Huang et al. [88]. Short dotted red line is Z45.

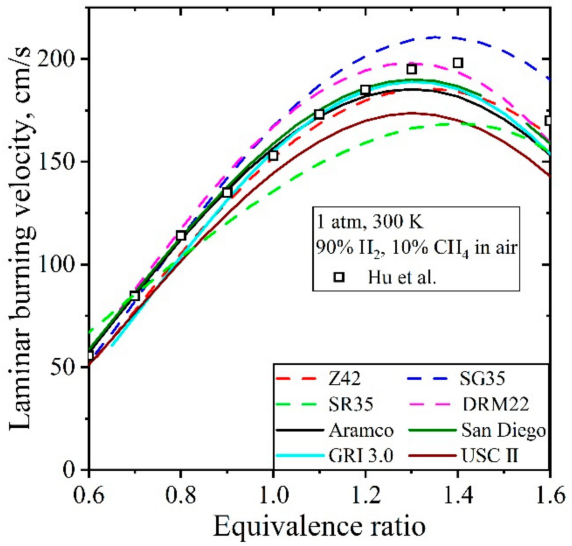

Figure A8. Laminar burning velocity for methane/hydrogen/air flames with 90% H_2. Initial gas mixture temperatures of 300 K and pressure 1 atm. Experimental data [33–36], represented by symbols, and modeling [7,9–11,16,30] represented by lines.

References

1. Burnham, A.; Han, J.; Clark, C.E.; Wang, M.; Dunn, J.B.; Palou-Rivera, I. Life-cycle greenhouse gas emissions of shale gas, natural gas, coal, and petroleum. *Environ. Sci. Technol.* **2011**, *46*, 619–627. [CrossRef] [PubMed]
2. Glassman, I.; Yetter, R.A. *Combustion*, 4th ed.; Elsevier: Amsterdam, The Netherlands, 2010.
3. Lu, T.F.; Law, C.K. Toward accommodating realistic fuel chemistry in large-scale computations. *Prog. Energy Combust. Sci.* **2009**, *35*, 192–215. [CrossRef]
4. Fiorina, B.; Veynante, D.; Candel, S. Modeling combustion chemistry in large eddy simulation of turbulent flames. *Flow Turbul. Combust.* **2015**, *94*, 3–42. [CrossRef]
5. Pope, S.B. Small scales, many species and the manifold challenges of turbulent combustion. *Proc. Combust. Inst.* **2013**, *34*, 1–31. [CrossRef]
6. Hilbert, R.; Tap, F.; El-Rabii, H.; Thevenin, D. Impact of detailed chemistry and transport models on turbulent combustion simulations. *Prog. Energy Combust. Sci.* **2004**, *30*, 61–117. [CrossRef]

7. Fischer, M.; Jiang, X. A chemical kinetic modelling study of the combustion of CH_4-CO-H-2-CO_2 fuel mixtures. *Combust. Flame* **2016**, *167*, 274–293. [CrossRef]
8. Fischer, M.; Jiang, X. An investigation of the chemical kinetics of biogas combustion. *Fuel* **2015**, *150*, 711–720. [CrossRef]
9. Fischer, M.; Jiang, X. An assessment of chemical kinetics for bio-syngas combustion. *Fuel* **2014**, *137*, 293–305. [CrossRef]
10. Dirrenberger, P.; Gall, H.L.; Bounaceur, R.; Herbinet, O.; Glaude, P.A.; Konnov, A.; Battin-Leclerc, F. Measurements of Laminar Flame Velocity for Components of Natural Gas. *Energy Fuels* **2011**, *25*, 3875–3884. [CrossRef]
11. Rashwan, S.S.; Nemitallah, M.A.; Habib, M.A. Review on premixed combustion technology: Stability, emission control, applications, and numerical case study. *Energy Fuels* **2016**. [CrossRef]
12. Tang, C.L.; Zhang, Y.J.; Huang, Z.H. Progress in combustion investigations of hydrogen enriched hydrocarbons. *Renew. Sustain. Energy Rev.* **2014**, *30*, 195–216. [CrossRef]
13. Taamallah, S.; Vogiatzaki, K.; Alzahrani, F.M.; Mokheimer, E.M.A.; Habib, M.A.; Ghoniem, A.F. Fuel flexibility, stability and emissions in premixed hydrogen-rich gas turbine combustion: Technology, fundamentals, and numerical simulations. *Appl. Energy* **2015**, *154*, 1020–1047. [CrossRef]
14. Ayed, A.H.; Kusterer, K.; Funke, H.W.; Keinz, J.; Striegan, C.; Bohn, D. Experimental and numerical investigations of the dry-low-NOx hydrogen micromix combustion chamber of an industrial gas turbine. *Prop. Power Res.* **2015**, *4*, 123–131. [CrossRef]
15. Brand, J.; Sampath, S.; Shum, F.; Bayt, R.; Cohen, J. Potential use of hydrogen in air propulsion. In Proceedings of the AIAA International Air and Space Symposium and Exposition: The Next 100 Years, Dayton, OH, USA, 14–17 July 2003; p. 2879.
16. Tang, C.L.; Huang, Z.H.; Law, C.K. Determination, correlation, and mechanistic interpretation of effects of hydrogen addition on laminar flame speeds of hydrocarbon-air mixtures. *Proc. Combust. Inst.* **2011**, *33*, 921–928. [CrossRef]
17. Eder, L.; Ban, M.; Pirker, G.; Vujanovic, M.; Priesching, P.; Wimmer, A. Development and Validation of 3D-CFD Injection and Combustion Models for Dual Fuel Combustion in Diesel Ignited Large Gas Engines. *Energies* **2018**, *11*, 643. [CrossRef]
18. Monsalve-Serrano, J.; Belgiorno, G.; Di Blasio, G.; Guzmán-Mendoza, M. 1D Simulation and Experimental Analysis on the Effects of the Injection Parameters in Methane–Diesel Dual-Fuel Combustion. *Energies* **2020**, *13*, 3734. [CrossRef]
19. Fraioli, V.; Beatrice, C.; Di Blasio, G.; Belgiorno, G.; Magliaccio, M. *Multidimensional Simulations of Combustion in Methane-Diesel Dual-Fuel Light-Duty Engines*; SAE Technical Paper 2017-01-0568; SAE: Warrendale, PA, USA, 2017.
20. Konnov, A.A.; Mohammad, A.; Kishore, V.R.; Kim, N.I.; Prathap, C.; Kumar, S. A comprehensive review of measurements and data analysis of laminar burning velocities for various fuel+air mixtures. *Prog. Energy Combust. Sci.* **2018**, *68*, 197–267. [CrossRef]
21. Ranzi, E.; Frassoldati, A.; Grana, R.; Cuoci, A.; Faravelli, T.; Kelley, A.P.; Law, C.K. Hierarchical and comparative kinetic modeling of laminar flame speeds of hydrocarbon and oxygenated fuels. *Prog. Energy Combust. Sci.* **2012**, *38*, 468–501. [CrossRef]
22. Metcalfe, W.K.; Burke, S.M.; Ahmed, S.S.; Curran, H.J. A hierarchical and comparative kinetic modeling study of C_1-C_2 hydrocarbon and oxygenated fuels. *Int. J. Chem. Kinet.* **2013**, *45*, 638–675. [CrossRef]
23. Li, Y.; Zhou, C.-W.; Somers, K.P.; Zhang, K.; Curran, H.J. The oxidation of 2-butene: A high pressure ignition delay, kinetic modeling study and reactivity comparison with isobutene and 1-butene. *Proc. Combust. Inst.* **2017**, *36*, 403–411. [CrossRef]
24. Zhou, C.-W.; Li, Y.; Burke, U.; Banyon, C.; Somers, K.P.; Ding, S.; Khan, S.; Hargis, J.W.; Sikes, T.; Mathieu, O.; et al. An experimental and chemical kinetic modeling study of 1,3-butadiene combustion: Ignition delay time and laminar flame speed measurements. *Combust. Flame* **2018**, *197*, 423–438. [CrossRef]
25. Group, T.C.M. C1-C3 Mechanism Version 1412. Available online: http://creckmodeling.chem.polimi.it/menu-kinetics/menu-kinetics-detailed-mechanisms/menu-kinetics-c1-c3-mechanism (accessed on 29 August 2018).
26. Curran, H.J. Developing detailed chemical kinetic mechanisms for fuel combustion. *Proc. Combust. Inst.* **2019**, *37*, 57–81. [CrossRef]
27. Turanyi, T.; Tomlin, A.S. *Analysis of Kinetic Reaction Mechanisms*; Springer: Berlin/Heidelberg, Germany, 2014.
28. Zettervall, N.; Fureby, C.; Nilsson, E.J.K. Small skeletal kinetic mechanism for kerosene combustion. *Energy Fuels* **2016**, *30*, 9801–9813. [CrossRef]
29. Zettervall, N.; Fureby, C.; Nilsson, E.J.K. A reduced chemical kinetic reaction mechanism for kerosene-air combustion. *Fuel* **2020**, *269*, 117446. [CrossRef]
30. Davidson, D.F.; Hanson, R.K. Interpreting shock tube ignition data. *Int. J. Chem. Kinet.* **2004**, *36*, 510–523. [CrossRef]
31. Goldsborough, S.S.; Hochgreb, S.; Vanhove, G.; Wooldridge, M.S.; Curran, H.J.; Sung, C.J. Advances in rapid compression machine studies of low- and intermediate-temperature autoignition phenomena. *Prog. Energy Combust. Sci.* **2017**, *63*, 1–78. [CrossRef]
32. Sung, C.-J.; Curran, H.J. Using rapid compression machines for chemical kinetics studies. *Prog. Energy Combust. Sci.* **2014**, *44*, 1–18. [CrossRef]
33. Ansari, A.; Egolfopoulos, F.N. Flame ignition in the counterflow configuration: Reassessing the experimental assumptions. *Combust. Flame* **2016**, *174*, 37–49. [CrossRef]
34. Law, C.K. Comprehensive description of chemistry in combustion modeling. *Combust. Sci. Technol.* **2005**, *177*, 845–870. [CrossRef]
35. Egolfopoulos, F.N.; Hansen, N.; Ju, Y.; Kohse-Hoinghaus, K.; Law, C.K.; Qi, F. Advances and challenges in laminar flame experiments and implications for combustion chemistry. *Prog. Energy Combust. Sci.* **2014**, *43*, 36–67. [CrossRef]
36. Goswami, M.; Derks, S.C.R.; Coumans, K.; Slikker, W.J.; O'liveira, M.H.D.; Bastiaans, R.J.M.; Luijten, C.C.M.; de Goey, L.P.H.; Konnov, A.A. The effect of elevated pressures on the laminar burning velocity of methane plus air mixtures. *Combust. Flame* **2013**, *160*, 1627–1635. [CrossRef]

37. Alekseev, V.A.; Naucler, J.D.; Christensen, M.; Nilsson, E.J.K.; Volkov, E.N.; de Goey, L.P.H.; Konnov, A.A. Experimental uncertainties of the heat flux method for measuring burning velocities. *Combust. Sci. Technol.* **2016**, *188*, 853–894. [CrossRef]
38. Chen, Z. On the accuracy of laminar flame speeds measured from outwardly propagating spherical flames: Methane/air at normal temperature and pressure. *Combust. Flame* **2015**, *162*, 2442–2453. [CrossRef]
39. Ranzi, E. A wide-range kinetic modeling study of oxidation and combustion of transportation fuels and surrogate mixtures. *Energy Fuels* **2006**, *20*, 1024–1032. [CrossRef]
40. Holley, A.T.; Dong, Y.; Andac, M.G.; Egolfopoulos, F.N. Extinction of premixed flames of practical liquid fuels: Experiments and simulations. *Combust. Flame* **2006**, *144*, 448–460. [CrossRef]
41. Holley, A.T.; You, X.Q.; Dames, E.; Wang, H.; Egolfopoulos, F.N. Sensitivity of propagation and extinction of large hydrocarbon flames to fuel diffusion. *Proc. Combust. Inst.* **2009**, *32*, 1157–1163. [CrossRef]
42. Franzelli, B.; Riber, E.; Cuenot, B. Impact of the chemical description on a Large Eddy Simulation of a lean partially premixed swirled flame. *Comptes Rendus Mécanique* **2013**, *341*, 247–256. [CrossRef]
43. Gu, X.J.; Haq, M.Z.; Lawes, M.; Woolley, R. Laminar burning velocity and Markstein lengths of methane-air mixtures. *Combust. Flame* **2000**, *121*, 41–58. [CrossRef]
44. Rozenchan, G.; Zhu, D.L.; Law, C.K.; Tse, S.D. Outward propagation, burning velocities, and chemical effects of methane flames up to 60 ATM. *Proc. Combust. Inst.* **2002**, *29*, 1461–1470. [CrossRef]
45. Lowry, W.; de Vries, J.; Krejci, M.; Petersen, E.; Serinyel, Z.; Metcalfe, W.; Curran, H.; Bourque, G. Laminar Flame Speed Measurements and Modeling of Pure Alkanes and Alkane Blends at Elevated Pressures. *J. Eng. Gas. Turbines Power* **2011**, *133*, 91501. [CrossRef]
46. Bosschaart, K.J.; de Goey, L.P.H. The laminar burning velocity of flames propagating in mixtures of hydrocarbons and air measured with the heat flux method. *Combust. Flame* **2004**, *136*, 261–269. [CrossRef]
47. Hu, E.J.; Li, X.T.; Meng, X.; Chen, Y.Z.; Cheng, Y.; Xie, Y.L.; Huang, Z.H. Laminar flame speeds and ignition delay times of methane-air mixtures at elevated temperatures and pressures. *Fuel* **2015**, *158*, 1–10. [CrossRef]
48. Frenklach, F.; Wang, H.; Yu, C.L.; Goldenberg, M.; Bowman, C.T.; Hanson, R.K.; Davidson, D.F.; Chang, E.J.; Smith, G.P.; Golden, D.M.; et al. GRI Mech 1.2. Available online: http://www.me.berkeley.edu/gri_mech (accessed on 1 August 2018).
49. Wang, H.; You, X.; Joshi, A.V.; Davis, S.G.; Laskin, A.; Egolfopoulos, F.; Law, C.K. USC Mech Version II. High-Temperature Combustion Reaction Model of H_2/CO/C1-C4 Compounds. Available online: http://ignis.usc.edu/USC_Mech_II.htm (accessed on 1 May 2007).
50. Chemical-Kinetic Mechanisms for Combustion Applications. Available online: http://combustion.ucsd.edu (accessed on 29 August 2018).
51. Kazakov, A.; Frenklach, F. DRM22. Available online: http://combustion.berkeley.edu/drm/ (accessed on 10 October 2018).
52. Smith, G.P.; Golden, D.M.; Frenklach, F.; Moriarty, N.W.; Eiteneer, B.; Goldenberg, M.; Bowman, C.T.; Hanson, R.K.; Song, S.; Gardiner, W.C.; et al. GRI-Mech 3.0. Available online: http://combustion.berkeley.edu/gri_mech/ (accessed on 29 October 2018).
53. Westbrook, C.K.; Dryer, F.L. Chemical kinetic modeling of hydrocarbon combustion. *Prog. Energy Combust. Sci.* **1984**, *10*, 1–57. [CrossRef]
54. Westbrook, C.K.; Dryer, F.L. Simplified reaction-mechanisms for the oxidation of hydrocarbon fuels in flames. *Combust. Sci. Technol.* **1981**, *27*, 31–43. [CrossRef]
55. Jones, W.P.; Lindstedt, R.P. Global reaction schemes for hydrocarbon combustion. *Combust. Flame* **1988**, *73*, 233–249. [CrossRef]
56. Seshadri, K.; Bai, X.S.; Pitsch, H.; Peters, N. Asymptotic analysis of the structure of moderately rich methane-air flames. *Combust. Flame* **1998**, *113*, 589–602. [CrossRef]
57. Fernandez-Tarrazo, E.; Sanchez, A.L.; Linan, A.; Williams, F.A. A simple one-step chemistry model for partially premixed hydrocarbon combustion. *Combust. Flame* **2006**, *147*, 32–38. [CrossRef]
58. Nikolaou, Z.M.; Chen, J.Y.; Swaminathan, N. A 5-step reduced mechanism for combustion of CO/H-2/H_2O/CH_4/CO_2 mixtures with low hydrogen/methane and high H_2O content. *Combust. Flame* **2013**, *160*, 56–75. [CrossRef]
59. Nikolaou, Z.M.; Swaminathan, N.; Chen, J.Y. Evaluation of a reduced mechanism for turbulent premixed combustion. *Combust. Flame* **2014**, *161*, 3085–3099. [CrossRef]
60. Abou-Taouk, A.; Sadasivuni, S.; Lorstad, D.; Eriksson, L.-E. Evaluation of global mechanisms for les analysis of sgt-100 dle combustion system. In Proceedings of the ASME Turbo Expo 2013: Turbine Technical Conference and Exposition, 3–7 June 2013. Number V002t04a036.
61. Smooke, M.D.; Giovangigli, V. Formulation of the premixed and nonpremixed test problems. In *Reduced Chemical Mechansims and Asymptotic Approximations for Methane-Air Flames*; Springer: New York, NY, USA, 1991; p. 384.
62. Bulat, G.; Fedina, E.; Fureby, C.; Meier, W.; Stopper, U. Reacting flow in an industrial gas turbine combustor: LES and experimental analysis. *Proc. Combust. Inst.* **2015**, *35*, 3175–3183. [CrossRef]
63. Ehn, A.; Petersson, P.; Zhu, J.J.; Li, Z.S.; Alden, M.; Nilsson, E.J.K.; Larfeldt, J.; Larsson, A.; Hurtig, T.; Zettervall, N.; et al. Investigations of microwave stimulation of a turbulent low-swirl flame. *Proc. Combust. Inst.* **2017**, *36*, 4121–4128. [CrossRef]
64. Larsson, A.; Zettervall, N.; Hurtig, T.; Nilsson, E.J.K.; Ehn, A.; Petersson, P.; Alden, M.; Larfeldt, J.; Fureby, C. Skeletal methane–air reaction mechanism for large eddy simulation of turbulent microwave-assisted combustion. *Energy Fuels* **2017**, *31*, 1904–1926. [CrossRef]

65. Zettervall, N.; Fureby, C. A computational study of ramjet, scramjet and dual-mode ramjet/scramjet combustion in a combustor with a cavity flameholder. In Proceedings of the AIAA 2018: 8th International Conference on Artificial Intelligence, Soft Computing and Applications, Melbourne, Australia, 24–25 November 2018.
66. Zettervall, N.; Nordin-Bates, K.; Nilsson, E.J.K.; Fureby, C. Large Eddy Simulation of a premixed bluff body stabilized flame using global and skeletal reaction mechanisms. *Combust. Flame* **2017**, *179*, 1–22. [CrossRef]
67. Niklas, Z.; Ekaterina, F.; Kevin, N.-B.; Heimdal, N.E.; Christer, F. Combustion LES of a multi-burner annular aeroengine combustor using a skeletal reaction mechanism for Jet-A air mixtures. In Proceedings of the 51st AIAA/SAE/ASEE Joint Propulsion Conference, American Institute of Aeronautics and Astronautics, Orlando, FL, USA, 27–29 July 2015. [CrossRef]
68. Zettervall, N.; Fureby, C.; Nilsson, E.J.K. Small skeletal kinetic reaction mechanism for ethylene-air combustion. *Energy Fuels* **2017**. [CrossRef]
69. Sher, E.; Refael, S. A simplified reaction scheme for the combustion of hydrogen enriched methane air flame. *Combust. Sci. Technol.* **1988**, *59*, 371–389. [CrossRef]
70. Refael, S.; Sher, E. Reaction-kinetics of hydrogen-enriched methane air and propane air flames. *Combust. Flame* **1989**, *78*, 326–338. [CrossRef]
71. Pitz, W.J.; Westbrook, C.K. Chemical-kinetics of the high-pressure oxidation of normal-butane and its relation to engine knock. *Combust. Flame* **1986**, *63*, 113–133. [CrossRef]
72. Frenklach, F.; Wang, H.; Yu, C.L.; Goldenberg, M.; Bowman, C.T.; Hanson, R.K.; Davidson, D.F.; Chang, E.J.; Smith, G.P.; Golden, D.M.; et al. GRI-Mech 1.2. Available online: http://combustion.berkeley.edu/gri_mech/new21/version12/text12.html (accessed on 29 August 2018).
73. Smith, G.P.; Golden, D.M.; Frenklach, M.; Moriarty, N.W.; Eiteneer, B.; Goldenberg, M.; Bowman, C.T.; Hanson, R.K.; Song, S.; Gardiner, W.C.; et al. *GRI 1.2*; GRI: Berkeley, CA, USA, 1999.
74. Wang, H.; Frenklach, F. Detailed reduction of reaction mechanisms for flame modeling. *Combust. Flame* **1991**, *87*, 365–370. [CrossRef]
75. Kazakov, A.; Frenklach, F. DRM19. Available online: http://combustion.berkeley.edu/drm/ (accessed on 29 August 2018).
76. Jaravel, T.; Riber, E.; Cuenot, B.; Bulat, G. Large Eddy Simulation of an industrial gas turbine combustor using reduced chemistry with accurate pollutant prediction. *Proc. Combust. Inst.* **2017**, *36*, 3817–3825. [CrossRef]
77. Chen, Y.L.; Chen, J.Y. Towards improved automatic chemical kinetic model reduction regarding ignition delays and flame speeds. *Combust. Flame* **2018**, *190*, 293–301. [CrossRef]
78. Goos, E.; Burcat, A.; Ruscic, B. *Extended Third Millenium Ideal Gas and Condensed Phase Thermochemical Database for Combustion with Updates from Active Thermochemical Tables*; Elke Goos: Remchingen, Germany, 2016.
79. ANSYS. *CHEMKIN-PRO 15151*; ANSYS: Canonsburg, PA, USA, 2016.
80. Goodwin, D.G.; Speth, R.L.; Moffat, H.K.; Weber, B.W. Cantera: An Object-Oriented Software Toolkit for Chemical Kinetics, Thermodynamics, and Transport Processes, 2.4.0. Available online: https://cantera.org/community.html#citing-cantera (accessed on 1 August 2018).
81. Kazakov, A. *Igdelay v1.0*; Princeton University: Princeton, NJ, USA, 2004.
82. Nilsson, E.J.K.; van Sprang, A.; Larfeldt, J.; Konnov, A.A. The comparative and combined effects of hydrogen addition on the laminar burning velocities of methane and its blends with ethane and propane. *Fuel* **2017**, *189*, 369–376. [CrossRef]
83. Park, O.; Veloo, P.S.; Liu, N.; Egolfopoulos, F.N. Combustion characteristics of alternative gaseous fuels. *Proc. Combust. Inst.* **2011**, *33*, 887–894. [CrossRef]
84. Wu, Y.; Modica, V.; Rossow, B.; Grisch, F. Effects of pressure and preheating temperature on the laminar flame speed of methane/air and acetone/air mixtures. *Fuel* **2016**, *185*, 577–588. [CrossRef]
85. Petersen, E.L.; Davidson, D.F.; Hanson, R.K. Ignition delay times of ram accelerator CH/O/Diluent mixtures. *J. Propuls. Power* **1999**, *15*, 82–91. [CrossRef]
86. Eubank, C.S.; Rabinowitz, M.J.; Gardiner, W.C.; Zellner, R. Shock-initiated ignition of natural gas-air mixtures. *Symp. (Int.) Combust.* **1981**, *17*, 1767–1773. [CrossRef]
87. Petersen, E.L.; Hall, J.M.; Smith, S.D.; de Vries, J.; Amadio, A.R.; Crofton, M.W. Ignition of lean methane-based fuel blends at gas turbine pressures. *J. Eng. Gas. Turbines Power Trans. ASME* **2007**, *129*, 937–944. [CrossRef]
88. Huang, J.; Bushe, W.K.; Hill, P.G.; Munshi, S.R. Experimental and kinetic study of shock initiated ignition in homogeneous methane-hydrogen-air mixtures at engine-relevant conditions. *Int. J. Chem. Kinet.* **2006**, *38*, 221–233. [CrossRef]
89. Versailles, P.; Watson, G.M.G.; Lipardi, A.C.A.; Bergthorson, J.M. Quantitative CH measurements in atmospheric-pressure, premixed flames of C_1-C_4 alkanes. *Combust. Flame* **2016**, *165*, 109–124. [CrossRef]
90. Le Cong, T.; Dagaut, P.; Dayma, G. Oxidation of natural gas, natural gas/syngas mixtures, and effect of burnt gas recirculation: Experimental and detailed kinetic modeling. *J. Eng. Gas. Turbines Power Trans. ASME* **2008**, 130. [CrossRef]
91. Goeckeler, K.; Krueger, O.; Paschereit, C.O. Laminar burning velocities and emissions of hydrogen-methane-air-steam mixtures. *J. Eng. Gas. Turb Power* **2015**, 137. [CrossRef]
92. Scholte, T.G.; Vaags, P.B. Burning Velocities of Mixtures of Hydrogen, Carbon Monoxide and Methane with Air. *Combust. Flame* **1959**, *3*, 511. [CrossRef]
93. McLean, I.C.; Smith, D.B.; Taylor, S.C. The use of carbon monoxide/hydrogen burning velocities to examine the rate of the CO + OH reaction. *Symp. Combust. Proc.* **1994**, *25*, 749. [CrossRef]

94. Krejci, M.C.; Mathieu, O.; Vissotski, A.J.; Ravi, S.; Sikes, T.G.; Petersen, E.L.; Kermones, A.; Metcalfe, W.; Curran, H.J. Laminar flame speed and ignition delay time data for the kinetic modeling of hydrogen and syngas fuel blends. *J. Eng. Gas. Turbines Power Trans. ASME* **2013**, *135*. [CrossRef]
95. Burbano, H.J.; Pareja, J.; Amell, A.A. Laminar burning velocities and flame stability analysis of H_2/CO/air mixtures with dilution of N_2 and CO_2. *Int. J. Hydrogen Energy* **2011**, *36*, 3232. [CrossRef]
96. Sun, H.; Yang, S.I.; Jomaas, G.; Law, C.K. High-pressure laminar flame speeds and kinetic modeling of carbon monoxide/hydrogen combustion. *Proc. Combust. Inst.* **2007**, *31*, 439. [CrossRef]